Theses and Dissertations

Fall 2014

Role of homolog CuZnSOD in baculovirus infection in insect cells

Bhakti Kishor Bapat
University of Iowa

Recommended Citation

Bapat, Bhakti Kishor. "Role of homolog CuZnSOD in baculovirus infection in insect cells." MS (Master of Science) thesis, University of Iowa, 2014.
https://doi.org/10.17077/etd.d8d5a83h

ROLE OF HOMOLOG CuZnSOD IN BACULOVIRUS INFECTION IN INSECT CELLS

by

Bhakti Kishor Bapat

A thesis submitted in partial fulfillment
of the requirements for the
Interdisciplinary Studies - Master of
Science degree in Biochemical
Engineering in the Graduate College of
The University of Iowa

December 2014

Thesis Supervisor: Professor David W. Murhammer

Graduate College

The University of Iowa

Iowa City, Iowa

CERTIFICATE OF APPROVAL

_____

MASTER'S THESIS

_____

This is to certify that the Master's thesis of

Bhakti K. Bapat

has been approved by the Examining Committee for the thesis requirement for the Interdisciplinary Studies - Master of Science degree in Biochemical Engineering at the December 2014 graduation.

Thesis Committee:

_____
David W. Murhammer, Thesis Supervisor

_____
Tonya Peeples

_____
Eric Nuxoll

To my parents, without them nothing would ever have been possible

ACKNOWLEDGMENTS

ABSTRACT

The baculovirus expression vector system (BEVS) is extensively used to produce recombinant proteins due to its high rate of expression. The major drawback of using this system is the early cell death (typically after 48-72 h post infection) that leads to decreased recombinant protein expression. Viral infection increases the production of reactive oxygen species (ROS) that are believed to contribute to this early cell death. Baculoviruses contain a Copper-Zinc Superoxide Dismutate (CuZnSOD) homolog gene that inactivates cellular CuZnSOD activity in insect cells by ~48 h post infection. Specifically, the CuZnSOD homolog inactivates the CuZnSOD enzyme by binding the copper chaperone, thereby leading to increased oxidative stress and presumably more rapid cell death. CuZnSOD activity during Wt-AcMNPV infection decreased to 0 in about 48-60 h post infection.

In this study the *Autographa californica* multiple nucleopolyhedrovirus (AcMNPV) modified to overexpress human CuZnSOD and Copper chaperone cassette (CCS) and devoid of the viral CuZnSOD homolog showed lower infectivity compared to Wt- AcMNPV infection. Futhermore, the addition of H_2O_2 to induce oxidative stress increased the infectivity of the modified AcMNPV, thereby supporting the premise that a minimal level of oxidative stress is required for improved infection. Further investigations are required to determine if this modified virus would be a better expression vector then the conventionally used baculovirus vectors.

iv

PUBLIC ABSTRACT

Baculoviruses are widely used with insect cells to express recombinant proteins. While the rate of recombinant protein expression can be very high in this system, the protein expression ceases within 2-3 days due to cell death resulting from the virus infection. Evidence suggests that oxidative stress is a major contributor to this cell death.

A baculovirus-encoded Copper-Zinc Superoxide Dismutate (CuZnSOD) homolog gene contributes to this oxidative stress. Specifically, the CuZnSOD homolog inactivates the CuZnSOD enzyme by binding to copper chaperone, thereby leading to increased oxidative stress and presumably more rapid cell death. Cell longevity potentially can be extended by increasing cellular antioxidant defenses, e.g., by removing the CuZnSOD homolog and overexpressing active CuZnSOD. The current research investigates the role of this homolog by studying modified baculovirus in which the CuZnSOD homolog gene has been removed and Human CuZnSOD is overexpressed.

TABLE OF CONTENTS

LIST OF TABLES

LIST OF FIGURES

LIST OF NOMENCLATURE

AcMNPV	*Autographa californica* multiple nucleopolyhedrovirus
APOX	Ascorbate Peroxidase
AvSOD	*Autographa californica* multiple nucleopolyhedrovirus with the viral CuZnSOD homolog gene disrupted by addition of lac-z gene
bp	Base pair
BV	Budded virus
CAT	Catalase
CCS	Copper chaperone protein
CHC	*Autographa californica* multiple nucleopolyhedrovirus with functional human Copper Zinc superoxide dismutase gene added viral copper zinc superoxide dismutase homolog gene deleted
CuZnSOD	Copper Zinc superoxide dismutase
czSOD	*Autographa californica* multiple nucleopolyhedrovirus with functional human copper zinc superoxide dismutase gene added
FBS	Fetal bovine serum
Gp64 .	Glycoprotein 64, it is found on the surface of the budded AcMNPV
GV	Granulovirus
hpi	Hours post infection
hSOD	Human superoxide dismutase
Kbp	Kilo base pair

MOI	Multiplicity of infection
NPV	Nucleopolyhedrovirus
OB	Occlusion body
OV	Occluded virus
PBS	Phosphate Buffer Solution
PCR	Polymerase chain reaction
pfu	Plaque forming units
ROS	Reactive oxygen species
Sf-21	*Spodoptera frugiperda* insect cell line isolated from ovarian tissue of fall army worm
Sf-9	*Spodoptera frugiperda* insect cell line from Sf-21, clone 9
SOD	Superoxide dismutase
$TCID_{50}$	Tissue culture infective dose for 50% to be infected
vSOD	Viral superoxide dismutase

CHAPTER 1- INTRODUCTION

Baculovirus:

In the early 1500s it was found that silkworms died due to some unknown illness and methods to alleviate the effects of this illness were developed. The introduction of the microscope allowed the direct observation of occlusion bodies in one type of disease. These bodies were polyhedron shaped, as shown in Figure 1. After the invention of the electron microscope in the late 1940s it was determined that rod shaped virions were present in these occlusion bodies and were responsible for the spread of this disease (Rohrmann, 2008).
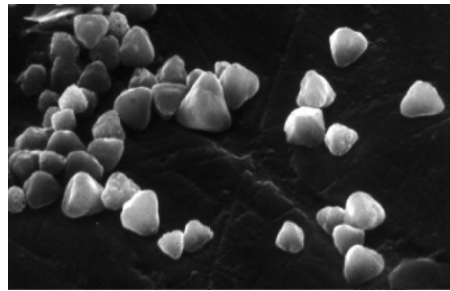
Figure 1: Baculovirus inclusion bodies.

The name baculovirus comes from baculo, which means 'rod shaped' and virus for virions. Baculoviruses infect insects and other invertebrates. These viruses have circular double stranded DNA genomes ranging from 80 to 180 kbp. The ability to occlude virions in a protein matrix is the characteristic of baculovirus.

1

Forms of Baculovirus:

Baculoviruses are classified as either granuloviruses (GV) or nucleopolyhedrovirus (NPV). GV produce granulin protein and have small particles containing one or two virions. NPV produce polyhedrin protein and larger particles with many virions. GVs are classified into three types: Type 1 GV viruses infect the midgut cells and subsequently the body's fat cells; Type 2 GVs infect the tracheal matrix or epidermis and have infections similar to those of NPVs and third type of GVs only infect the midgut tissues. NPVs are mainly found in two forms, budded virions (BV) and occluded virions (OV) and are generally more infectious then GVs.

Baculovirus infection process:

Transfer of the infection from one insect to another insect is carried out by the OVs, while BVs spread the infection from one cell to another inside the insect. Baculovirus infection within insects spreads when viral polyhedra are ingested by insects in their larval stage. These polyhedra pass through the digestive tract of the larvae and in the midgut region the alkaline pH dissolves the polyhedrin protein to release the OVs through the peritrophic membrane of the midgut and infect the epithelial cells of the midgut. Following this the virus starts replicating, producing BVs which are released into the circulatory system to spread the infection throughout the larvae. As the infection proceeds, BV production reduces and new nucleocapsids get incorporated in polyhedra. The total infection time ranges from approximately 5-7 days. Throughout the stages of infection the host insect goes through the following phases. During the first phase its skin swells and changes luster. In the second stage, its cuticle darkens and musculature disintegrates and

the larva becomes a sac of milky fluid. Finally, in the last stage, this larva bursts and releases polyhedral particles which are consumed by other insects. During the entire infection process approximately ten generations of virus are produced and approximately 25% of the larvae dry body weight consists of polyhedra (O'Reilly *et al.,* 1994).

Baculovirus Expression Vector System and its advantages over other expression systems:

Microbial expression systems have been widely used for recombinant protein production. The most famous examples of this is the production of simple proteins, e.g., insulin, using *Escherichia coli* and the production of bovine growth hormone using *Saccharomyes cervisiae* (Butler, 2005; Swartz, 2001). Many complex proteins, such as functional monoclonal antibodies or highly glycosylated proteins, require post translational processing for which the metabolic machinery is only available in higher eukaryotic cells or mammalian cells (Butler, 2005). While mammalian cells are the best to produce these proteins, they are also more costly for large scale production and can also lead to immune reactions when used in production of therapeutics. Another way of getting proteins is by extracting them from plants or animals directly, but that makes the process very expensive and leads to the sacrifice of many animals. Also, this method of production requires very difficult protein isolation from a plant or animal.

The baculovirus expression vector system (BEVS) was developed in the 1980s. This system can be used to express proteins in insect cell lines and produce valuable and functional proteins that are similar to mammalian cell proteins. Proteins produced by the BEVS can reduce the production time, as it takes less time to obtain a recombinant

www.manaraa.com

Autographica californica multiple nucleopolyhedrovirus (AcMNPV) for expressing a protein. Thus, the BEVS provides an intermediate approach between microbial and mammalian expression systems that is cost and quality effective. However, a major, problem with the BEVS is the production of excess reactive oxygen species (ROS) e.g. superoxide radical ($O_2^{\bullet-}$) and hydroperoxide radical ($^{\bullet}OH$) resulting in oxidative stress following viral infection of the cell. These oxidative stresses result in earlier cell death that reduces protein production.

Other Baculovirus Application:

Extensive use of chemical pesticides have resulted in the reduction of soil fertility, adverse health effects in humans and other animals, and increased insecticide resistance of insects. Thus, the use of baculoviruses as a part of Integrated Pest Management strategy is an attractive approach (Murhammer, 1996). Some of the baculoviruses that have been registered for use as pest control agents in the United States are: (i) *Lymantria dispar* MNPV (LdMNPV) for gypsy moth control, (ii) *Spodoptera exigua* NPV (SeNPV) for beet armyworm control, (iii) *Autographa californica* MNPV (AcMNPV) for alfalfa looper control and (iv) *Anagrapha falcifera NPV* (AfNPV) for control of lepidopteran species (Murhammer, 1996).

Baculovirus used as Expression Vector:

The baculovirus infection in cell culture can be split into three phases. Early phase or the reprogramming of the cells for virus replication followed by the late phase for production of BV and then the very late phase for OV production.

4

The early phase lasts for about the first six hours post infection (hpi). During this time the cells undergo significant changes, e.g., cytoskeleton re-arrangements, host chromatin dispersion within the nucleus and cell enlargement. These changes occur primarily due to new proteins expressed following viral infection. The late phase lasts from 6 hpi to approximately 20-24 hpi. This stage mainly accounts for BV production. The very late phase begins at approximately 20 hpi. The production of OVs mainly occurs in this phase and can be marked by the presence of occlusion bodies in the nucleus. Polyhedra-occlusion bodies have a crystalline nature and tend to give a highly refractive appearance to the group of infected cells or plaques.

The two most commonly used baculoviruses are *Bombyx mori* nucleopolyhedrovirus (BmNPV) and *Autographica californica* multiple nucleopolyhedrovirus (AcMNPV). Both of these viruses have a genome of approximately 130 kbp. The polyhedrin gene (polh) is expressed at very high levels during a separate and final phase of infection and this gene product is found to be nonessential for virus replication in cell culture (Smith *et al.*, 1983). Thus, the first recombinant baculovirus was developed by replacing the polh gene with a hetrogenous gene under the control of the polh promoter (Miller *et al.*, 1983b; Smith *et al.*, 1983b; Pennock *et al.*, 1984; Maeda *et al.*, 1985) and this is still used for most baculovirus expression vectors. This is also due to the fact that the polyhedron gene has a very strong promoter, leading to the accumulation of recombinant protein to levels as high as 50% of the total cell protein (O'Reilly *et al.*, 1994). Also, expression vectors have been developed with multiple copies of this promoter that can be used to simultaneously express several recombinant proteins (Belyaev *et al.*, 1995).

Moreover, the rod shape of the nucleocapsids of baculovirus can accommodate large viral DNA genomes, thereby allowing for DNA insertions at least as large as 15 kbp (O'Reilly *et al.*, 1994). Baculovirus vectors are relatively simple to use as they are independent of helper-virus. Construction of recombinant baculovirus is easier than cloning and isolating stable cell lines and they do not infect mammalian cells, therefore providing a much safer expression system (O'Reilly *et al.*, 1994).

Insect Cell Lines:

Insect cell lines have intermediate properties between mammalian cell lines and bacterial cell lines. Insect cells can perform post transitional protein folding like mammalian cells. However, it has been recognized that the protein processing pathways of insect cell lines differ from mammalian cell lines. For instance, the N- and O-linked glycosylation happens in a fundamentally different manner (Coleman *et al.,* 1997). Furthermore, protein production is dependent on the insect cell line, some insect cell lines simply may not be able to produce a functional protein, while others may be able to successfully carry out the protein processing (Harrison and Jarvis, 2007a). The three most commonly used insect cell lines for baculovirus expression are BTI-TN-5B1-4 (Tn-5; High Five cells), which are derived from the eggs of *Trichopulsia ni*, Sf-21 cells, which were heterogeneously derived from pupal ovarian tissue of *Spodoptera frugiperda*, and Sf-9 cells, which were cloned from the Sf-21 cell line to maximize β-galactosidase production during baculovirus expression (Wang *et al.,* 1992). The Sf-21 and Sf-9 cell lines are most commonly used for transfection, viral amplification and protein expression while Tn-5 are primarily used for protein expression (Murhammer, 2007b).

Oxidative Stress:

A major drawback of using baculovirus for producing recombinant proteins is that the infection leads to early cell death that ceases the protein production. AcMNPV contains the p35 gene encoding a stoichiometric inhibitor of active caspases that blocks apoptosis and therefore extends the life span of the cell (Miller *et al.*, 1998); the cells, however still undergo necrotic cell death due to infection (Wang *et. al.*, 2001a). Many cases have been reported where virally infected mammals and cells have shown higher oxidative stress (Wang *et. al.*, 2001a). Mice infected with influenza virus exhibited increased levels of superoxide radical ($O_2^{\bullet-}$) due to higher xanthine oxidase activity, but the mice were protected from lethal infection by simply injecting pyran copolymer conjugated superoxide dismutase (SOD) that removed the superoxide radical to form H_2O_2 (Oda *et al.*, 1989).

Leporipoxvirus encodes a CuZnSOD homolog gene which is shown to inhibit cellular CuZnSOD activity (Teoh *et al.*, 2002). Baculovirus also contains a CuZnSOD homolog gene (Tomalski *et al.*, 1991). Thus, it can be hypothesized that baculovirus CuZnSOD homolog inhibits CuZnSOD activity in insect cells. Thus, deleting the CuZnSOD homolog gene should result in infected cells that retain CuZnSOD activity, thereby reducing oxidative stess following virus infection, and extending cell life.

Overview:

This thesis is focused on the investigation of role played by viral CuZnSOD homolog during baculovirus infection. Chapter 2 explains the role of oxidative stress, its generation and action of various cellular defenses and strategies to reduce infection-induced oxidative stress. Chapters 3 and 4 discuss the current research work conducted in implementing the

strategies for reduction of oxidative stress including the methods and materials involved in

performing these experiments and the results and discussion. Finally, Chapter 5 contains

conclusions and suggestions for future work.

CHAPTER 2 - LITERATURE REVIEW

Generation and Effects of reactive oxygen species (ROS):

Reactive oxygen species (ROS) are entities containing one or more reactive oxygen atoms. ROS are produced throughout the cell due to a range of metabolic activities. O_2 sometimes undergoes univalent pathways of reduction, thereby resulting in the intermediate ROS. Approximately 1-2% of the O_2 gets converted to $O_2^{\bullet-}$ in the electron transport chain through a single electron transfer (Boveris and Chance, 1973) and is shown in Figure 2.
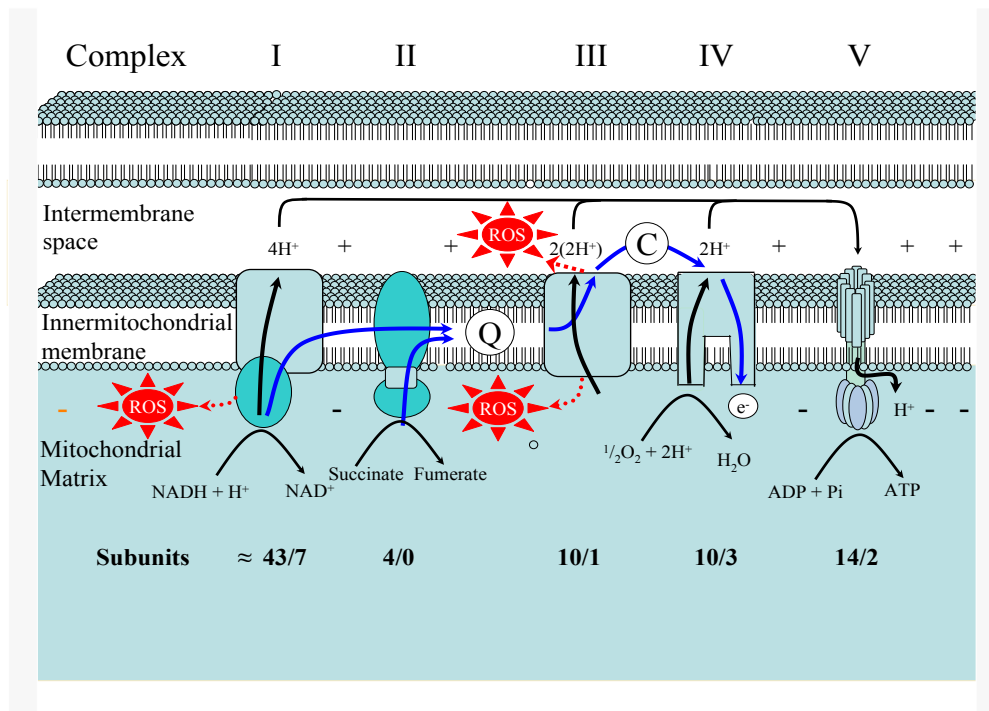
Figure 2: Generation of ROS by the electron transport chain located in mitochondria.

The pathway to form water from oxygen, intermediately forming superoxide radical ($O_2^{\bullet-}$), hydrogen peroxide (H_2O_2) and hydroxyl radical ($^{\bullet}OH$), is shown by Equation 1. The overall conversion of oxygen to water is given by Equation 2

$$O_2 \xrightarrow{+e^-} O_2^{\bullet-} \xrightarrow{+e^-} H_2O_2 \xrightarrow{+e^-} HO^{\bullet} \xrightarrow{+e^-} H_2O \qquad (1)$$

$$O_2 + 4e^- + 4H^+ \rightarrow 2H_2O \qquad (2)$$
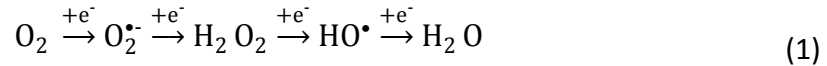
Under normal conditions the majority of the O_2 consumed by aerobic cells is reduced to H_2O by the transfer of four electrons through the mitochondrial electron transport chain as shown in Equation 2 and 1-2% of the O_2 receives only 1 electron to produce $O_2^{\bullet-}$ as shown in Equation 1. However, the host cell antioxidant enzymes generally are effective in removing this $O_2^{\bullet-}$. During pathogenic conditions, e.g., viral infection the activity of these antioxidants is hampered thereby resulting in increased ROS in the cells and thus an increase in oxidative stress. ROS are also produced in the nuclear membrane, plasma membrane and in the cytoplasm through the action of cytochrome b, NADPH oxidase and xanthine oxidase.

Peroxisomes are major production sites of H_2O_2, which is produced as a byproduct of oxidase catalyzed reactions. H_2O_2 can diffuse across biological membranes, but $O_2^{\bullet-}$ can only cross biological membranes if an appropriate ion channel is present. $O_2^{\bullet-}$ and H_2O_2 generally have poor reactivity in aqueous medium, but when catalyzed by iron can undergo a Haber-Weiss reaction to produce hydroxyl ions. These hydroxyl ions can also be formed in the presence of copper ion as shown in Equations 3, 4 and 5:

10

$$O_2^{\bullet-} + H_2O_2 \rightarrow O_2 + HO^{\bullet} + OH^-$$ (3)

$$Fe^{2+} + H_2O_2 \rightarrow Fe^{3+} + HO^{\bullet} + OH^-$$ (4)

$$Cu^+ + H_2O_2 \rightarrow Cu^{2+} + HO^{\bullet} + OH^-$$ (5)
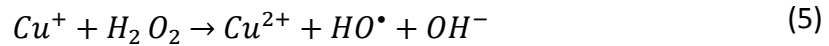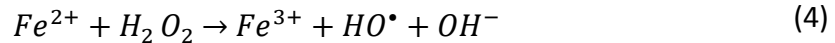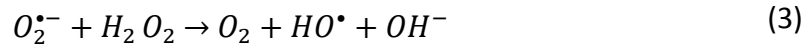
Small amounts of ROS are required for functions such as hydrolylation of aliphatic and aromatic compounds, but the accumulation of ROS leads to protein degradation, disintegration of nucleic acids and formation of lipid peroxides (Boveris and Chance, 1973; Jamieson, 1989). The protein peroxidation process is similar to lipid peroxidation forming alkoxyl and peroxyl radicals, e.g., H_2O_2 or $O_2^{\bullet-}$ react with the thiol group on cysteine or methionine and $^{\bullet}OH$ reacts with tryptophan to form peroxyl radicals (Halliwell and Gutteridge, 2007). Lipid peroxidation causes degradation of phospholipids leading to leaky membranes and eventual cell death (Buettner, 2011). Oxidized proteins are often rendered non-functional and hence get decomposed by proteinases. The mechanism of lipid peroxidation is shown in Figure 3.
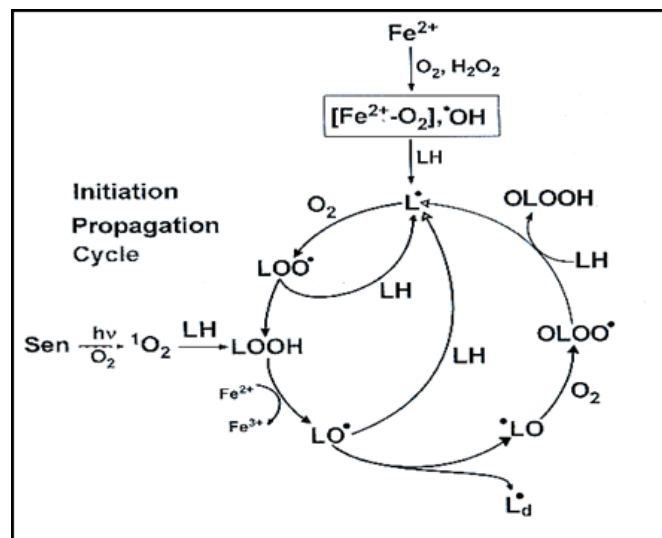
Figure 3: Mechanism of lipid peroxidation (Buettner, 2011).

Protein oxidation due to ROS is a major issue, especially when transport proteins and receptor proteins are oxidized (Boveris and Chance, 1973). These proteins are responsible for the active transport of essential ions and for maintaining a proper cell volume; thus, their alteration can lead to altered cell functions.

Antioxidant defenses of the cell:

ROS are removed from the cell by antioxidants like superoxide dismutases (SODs), catalase (CAT) and peroxidases like Glutathione peroxidase (GPX) in mammalian cells and Ascorbate peroxidase (APOX) in insect cells. SODs convert $O_2^{\bullet-}$ to H_2O_2, and CAT/ peroxidase convert H_2O_2 to H_2O. Cells mainly have two types of SODs Manganese Superoxide Dismutase (MnSOD) and Copper Zinc Superoxide Dismutase (CuZnSOD). Equation 6 shows an overview of the role of antioxidants in converting $O_2^{\bullet-}$ to H_2O.

$$O_2 \rightarrow O_2^{\bullet-} \xrightarrow{\overset{Superoxide}{dismutase}} H_2O_2 \xrightarrow{Peroxidases/Catalase} H_2O \qquad (6)$$
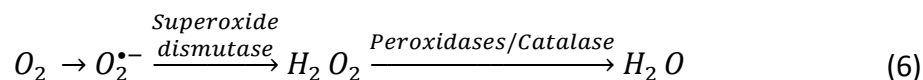
It is observed that Sf-21 and Sf-9 cells only show APOX activity, while Tn-5 cells show both CAT and APOX activity (Wang *et. al.*, 2001a). The antioxidant defense reaction mechanism in catalyzing $O_2^{\bullet-}$ to is explained in Equations 7, 8 and 9. Equations 7 and 8 illustrate the reaction mechanism for SOD reactions and Equation 9 explains the pathway for peroxidase and catalase reactions.

$$M^{(n+1)+} - SOD + O_2^{\bullet-} \rightarrow M^{n+} - SOD + O_2^{\bullet-} \qquad (7)$$
$$M^{n+} - SOD + O_2^{\bullet-} + 2H^+ \rightarrow M^{(n+1)+} - SOD + H_2O_2 \qquad (8)$$
$$2H_2O_2 \rightarrow 2H_2O + O_2 \qquad (9)$$
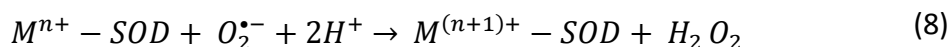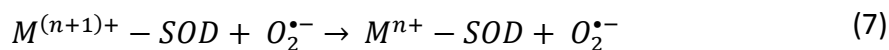
The effect of MnSOD overexpression of had been investigated in Sf-9 and Tn-5 cells by infecting with a recombinant AcMNPV expressing MnSOD under the control of the IE1 viral promoter. Overexpression of MnSOD in Tn-5B1-4 led to a decrease in protein and lipid oxidation, but showed no significant change in Sf-9. Alternatively, it was proposed that Ascorbate peroxidase or Catalase (APOX/CAT) imbalance in comparison with SODs may also have resulted in oxidative damage. Co-expression of MnSOD and APOX/CAT have led to enhanced protection from oxidation damage caused by viral infection (Wang *et al.,* 2004). The decreased MnSOD activity in mammalian cells following viral infection supports the hypothesis that pathological conditions hamper antioxidant defenses in cells, thereby resulting in increased oxidative stress (Lieven *et al.,* 2008). To regulate the ROS species, cells also use antioxidants like vitamin E and vitamin C (Boveris and Chance, 1973), but they are not as effective as antioxidant enzymes.

The other antioxidant enzyme, CuZnSOD it is a 32KDa dimeric protein. It is found in almost all eukaryotic cells and is found throughout in the cell. It is mainly located in lysosomes, peroxisomes, nuclei and in the space between the inner and outer mitochondrial membrane where it acts as an initial defense. Figure 4 shows the actives sites of the CuZnSOD enzyme (Tainer, 1983).
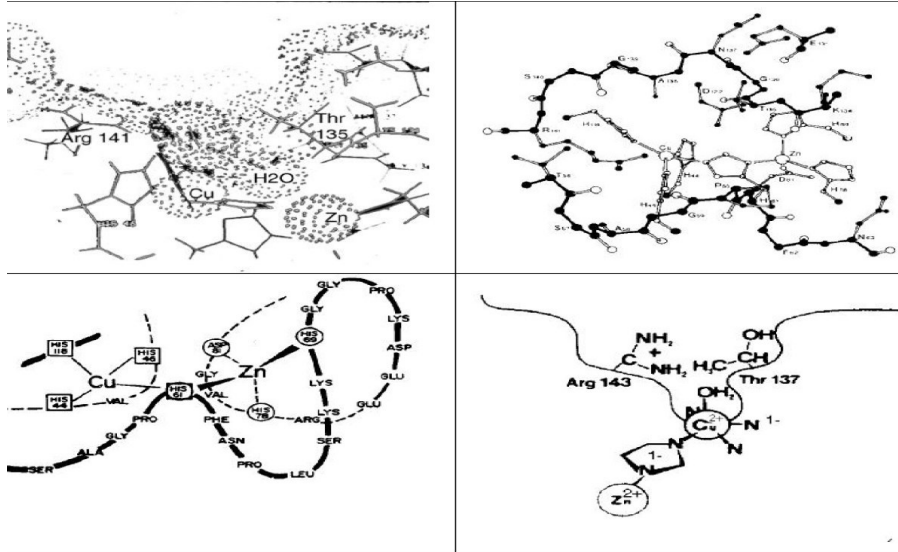
Figure 4: Four representations of CuZnSOD's active site (Tainer, 1983).

MnSOD and CuZnSOD are both metallochaperones. Manganese (Mn) transporter is required in yeast to deliver Mn to MnSOD, however the need for transporter can be overcome by increasing the concentration of Mn in the medium (Luk *et al.,* 2001). Similar studies have been done with CuZnSOD and it was found that toxicity increased by increasing the Copper (Cu) concentration in medium; thus, Cu cannot be incorporated into CuZnSOD just be increasing concentration and a copper chaperone (CCS) is required for incorporating Cu in CuZnSOD and thus is critical for CuZnSOD activity (Wong *et al.,* 2000).

Viral CuZnSOD Homolog:

Baculoviridae and Poxviridae families contain SOD homologs. The eukaryotic CuZnSOD is about 50% homologous to AcMNPV CuZnSOD homolog in total sequence identity and key amino acid residues (Tomalski *et al.,* 1991). Poxviruses have been shown to have amino acid substitutions that render them inactive, but these CuZnSOD homologs

14

show the capacity to bind to the chaperone for SOD (CCS) thus forming protein decoys that retain selective binding capacity to cellular CCS and thus interfer with the metallation reactions in cellular CuZnSOD (Teoh *et al.,* 2003)

Strategy for increasing the cellular CuZnSOD activity:

The analyses discussed in the previous sections suggested an approach to increase the cellular CuZnSOD activity the following analysis should be undertaken.

- AcMNPV should be modified to overexpress human CuZnSOD and delete the CuZnSOD homolog gene.
- Evaluate the effectiveness of the modified AcMNPV in a comparative study against wild type AcMNPV

CHAPTER 3 - ROLE OF BACULOVIRUS INFECTION- MATERIALS AND METHODS

Introduction:

Existing reviews have shown that the existence of viral CuZnSOD homolog might be an important requirement for spread of viral infection. It has been hypothised that a certain amount of oxidative stress is required for a viral infection, but its exact role has not yet been determined. To determine the role of oxidative stress and its relation with viral CuZnSOD homolog, an AcMNPV without the CuZnSOD homolog is needed. Furthermore, overexpressing human CuZnSOD and the copper chaperone would provide additional antioxidant capabilities. To this end, various recombinant viruses were developed by Dr. Donald Jarvis of University of Wyoming as discussed in the virus techniques section.

Cell culture:

Regular Maintenance

Sf-21 cells were acquired from Dr. Bonning's Lab (Iowa State University) and were grown regularly in Sf-900 II SFM (Invitrogen, Carlsbad, CA). Sterilized 125 mL Erlenmeyer flasks were used to grow cells with working volume of 20 mL. They were incubated in an orbital shaker incubator (Thermo Scientific, Waltham, MA) maintained at 27 ^{0}C with a rotational speed of 140 rpm. When the cell culture reached a density of 3-4×10^6 cell/mL, they were subcultured to cell density of 0.8×10^6 cell/mL using fresh medium. These cells were also sub-cultured in 25 cm^2 tissue culture flasks (T-25) in a ratio of 1 part of cells to 10 parts of medium every week for backup purposes and kept in incubator at 27 ^{0}C. Liquid nitrogen was used for long term storage and maintenance of these cells.

Cell density and viability were determined using a hemacytometer (Nikon, Melville, NY) with the trypan blue dye exclusion method. A manual count of viable and dead cells was performed to determine the cell density and percent cell viability. A hemacytometer is a glass plate with an etched grid in the middle as shown in Figure 5.
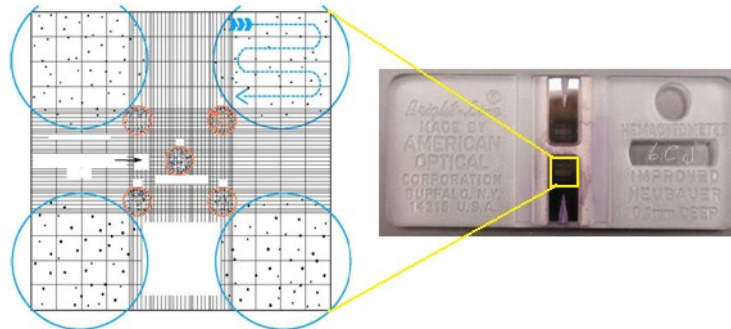
Figure 5: Schematic of Hemacytometer grid with the cell count areas.

This procedure works on the basic principle of differentiating between living and dead cells using trypan blue dye. Trypan blue dye stains the dead cells. Dead cells have leaky cell membranes that allow the dye to enter the cytoplasm, thereby staining it blue while the live cells resist the dye from entering, thus remaining colorless.

Cells are mixed with trypan blue with a certain dilution factor, and then this cellular suspension is filled in a counting chamber that is formed by the assembly of hemacytometer and cover glass. Cover glass covers the grid area and is kept on the cover glass support. These supports are provided on both the sides of the grid. Cellular suspension is filled in the counting chamber, which contains a 10 μL sample using a micro pipette. Cells are counted in the four side chambers marked by circles in Figure 5. The area

17

of this count square is 1mm^2 and the depth of this counting chamber is 0.1 mm, thus the volume is 0.1 mm^3. Thus the cell density in this chamber can be estimated using Equation 10.

$$N_t = \frac{Cf_d}{4 \times 1 \times 10^{-4} mL} \qquad (10)$$

Where,

N$_t$ = Viable Cell Density, cell/mL

C= Viable cells counted

f$_d$= Dilution factor

For viability calculations, the total number of live cells from all the four cell count areas is divided by the total number of cells in all those four cell count areas.

Thawing cells

Long term storage of cells can be done using liquid nitrogen. The cells remain stable in liquid nitrogen for a long time with minimal damage due to freezing. These cells can be thawed and brought to normal cell growth for cell culture. Cells are kept in 1 mL vials in nitrogen freezer. Cell growth medium supplemented with 10% v/v of Dimethyl Sulphoxide Solution (DMSO) and 10% FBS (v/v) is used to freeze cells. DMSO prevents formation of ice crystals during freezing, but it is also toxic to cells at room temperature. Thus, when the cells are thawed they have to be quickly subcultured to remove the DMSO.

18

A cell vial is removed from the liquid nitrogen freezer and transferred to warm water to quickly thaw the cells. These are then transferred to a 25 cm^2 tissue culture flask filled with 4 mL of medium enriched with 10% FBS. These cells are handled carefully and kept in an incubator at 27 ^{0}C for 1-2 hours and then observed under a light microscope to determine how many cells are attached to the bottom of the flask and therefore perceived to be viable. Once the cells are attached to the bottom the medium is replaced by fresh medium and the cells incubated at 27 ^{0}C for 24 h and then the medium is changed again. Note that only the medium is replaced, i.e., the cells remain attached to the flask surface. This process is repeated until the cells reach 90% confluence, and then they are sub-cultured into new tissue culture flasks. The sub-culturing into a new flask utilizes 1 mL cell suspension and 3 mL fresh medium. Once the cells begin growing normally, they are then slowly adapted to serum free medium. This involves reducing the FBS concentration by half at each subsequent subculture from 10% to 5% and then serum free SFM until they start growing naturally. After the cells are adapted to SFM, they are sub-cultured in shaker flasks at 0.8×10^6 cell/mL (O´Reilly *et al.,* 1994).

Virus Techniques:

The modified AcMNPV viruses used in this study are described in Table 1.

Table 1: Recombinant Baculoviruses used in this project.

Baculovirus Name	Baculovirus description
Wt	Wild type AcMNPV
czSOD	Virus overexpressing human CuZnSOD gene under the control of IE1 promoter
AvSOD	Viral CuZnSOD homolog gene disrupted by Lac-z gene insertion (Tomalski *et al.,* 1991).
CHC	Virus overexpressing human CuZnSOD and copper chaperone cassette under IE 1 promoter with CuZnSOD homolog gene removed
CHCpp1	New re-developed virus over expressing cassette of human CuZnSOD and copper chaperone under IE 1 promoter and with CuZnSOD homolog gene removed.

czSOD virus was developed by combining amplified pAcP(+)DIE1 with purified viral

DNA by standard homologous recombination. CHC virus was developed by using pBSP-

HindIII-LX17 plasmid obtained from Dr. Rollie Clem's lab and deleting the fragment

20

between Xho-1 and Nde-1 to obtain removal of CuZnSOD homolog. pAcp(+)DIE1 CuZnSOD/CCS plasmid was amplified and added to the deleted plasmid by the standard homologous recombination method. The verification was done by isolating white occ+ plaques. For making the CHCpp1 virus the viral CuZnSOD homolog knocked out virus with a replaced lac Z marker was linearized using the unique site Bsu36I. This was then linearized and amplified using PCR and then genomic DNA prepared. New transfer vector pBSP-Hind3-LX17 was carefully mapped and the Pac1 to fragment Nde 1 was deleted. pAcp(+)DIE1 CuZnSOD/CCS plasmid.was amplified and added toPac1 and Nde1 blunt ends. This product was then used to replace viral CuZnSOD orf in pBSP-Hind3-LX17. White plaques of occ+ were the isolated and verified with PCR. The complete viral gene map is given is Figure 6.
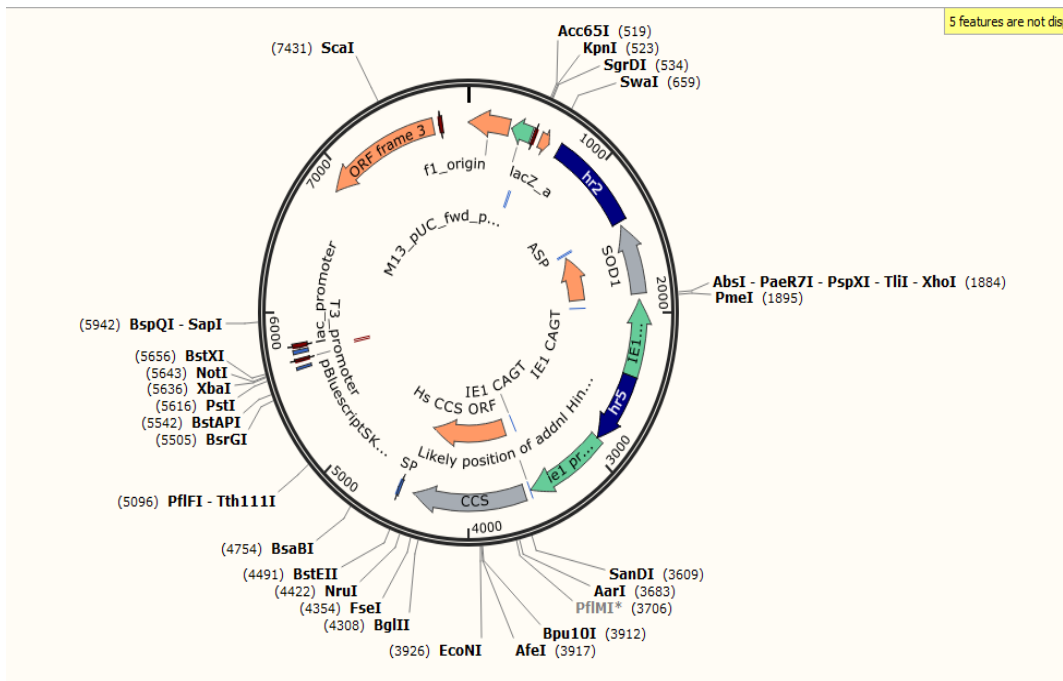
Figure 6: Circular map of recombinant AcMNPV DNA with human CuZnSOD/ CCS cassette under IE1 promoter and deletion of CuZnSOD homolog gene.

Virus Amplification

Virus amplification was conducted with the Sf-21 cell line. To produce 100 mL of viral stock, Sf-21 cells were cultured in 500 mL sterilized Erlenmeyer flasks in medium supplement with 10% FBS. The FBS was added to enhance virus stability during long term storage. When the cells reached a density of $1.5\text{-}2 \times 10^6$ cell/mL they were infected with virus at a multiplicity of infection (MOI- further detailed explanation of MOI is given in upcoming sections) of 0.1. Cell density and viability were determined daily. When the viability decreased to ~75%, the cell broth was sterilely centrifuged for 5 min at 1000 g. The cell pellet was discarded and the supernatant was collected and stored at 4 ^{0}C (O´Reilly *et al.,* 1994).

Virus Titration

Determining the concentration of virus is called virus titration. This can be performed using endpoint dilution assay. The determination of viral titer by endpoint dilution involves inoculation of multiple cultures with different virus dilutions. This technique estimates the dilution of virus that would infect 50% of the cultures to get the tissue culture infectious dose ($TCID_{50}$/mL), this is then converted to plaque forming units (pfu/mL) (O´Reilly *et al.*, 1994).

For performing this assay, serial dilutions of viral stock from 10^{-1} to 10^{-9} were prepared in medium. A solution of Sf-21 cells in medium at concentration of 10^5 cell/mL was prepared. A 180 µL/well of cell solution was inoculated in a 96 well plate, with the 8 columns representing serial dilution and the 12 rows represented number of samples per dilution. Generally, 20 µL/well of virus solutions ranging from 10^{-3rd} to 10^{-9th} dilution were

22

added to each row with one row consisting of control uninfected cells. It was then incubated for 10 days at 27 ^{0}C. The wells were checked under a light microscope, every day after the 4th day for signs of infection. The infected wells were marked positive and at the end of 10 day period the infected and uninfected wells were summarized. Figure 7 shows the general schematic of a final count of infected wells after a 10 day infection.
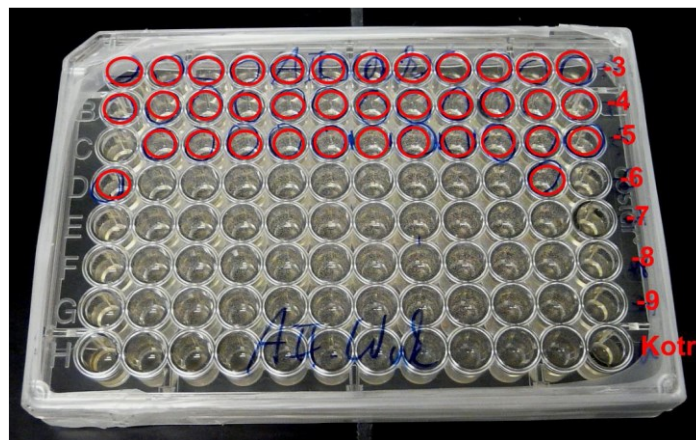
Figure 7: Endpoint dilution technique.

The titer was then estimated using an Excel worksheet program shown in

APPENDIX B

SAMPLE VIRUS TITER CALCULATION

Table given in Appendix. The calculations used in the worksheet were performed as follows. First, $TCID_{50}$ was calculated, $TCID_{50}$ corresponds to the dilution that leads to 50% of infected wells. This was calculated by interpolation as a proportional distance (PD) between two dilutions where first dilution shows above 50% infection positive wells (more than 6 wells) with infection, this is the upper response and the consecutive lower dilution shows number of positive wells less the 50% (less than 6 wells) infection positive wells. This is given in Equation 11 (O´Reilly *et al.,* 1994).

$$PD = \frac{A - 50}{A - B} \tag{11}$$

Where,

PD= Proportional distance

A=percent response greater than 50%

B= percent response less than 50 %

$TCID_{50}$ can then be calculated using Equation 12.

$$TCID_{50} = 10^{\log D_{50} - PD} \tag{12}$$

Where,

D_{50}= the dilution giving a response greater than 50%

The virus titer is estimated as pfu/mL as given by Equation 13. The multiplicity of infection (MOI) of a virus is the ratio of infectious virus particles (i.e., pfu) to cells. The fraction of cells infected with specific number of baculovirus can be predicted through the Poisson distribution given in Equation 14 and 15.

$$pfu = 0.69 \times TCID_{50} \tag{13}$$

$$F(n_v, MOI) = \frac{MOI^{n_v} e^{-MOI}}{n_v!} \tag{14}$$

This can also be rewritten as:

$$F(n_v, MOI) = 1 - e^{-MOI} \tag{15}$$

Where,

F (n_v,MOI) = Fraction of cells infected with n_v viruses at a given MOI;

n_v= Number of viruses that infect one cell

Characterizing the Modified virus:

The CHC virus was obtained from Elena Bond's previous research (Table 1); this was initially developed in 2006 in the Don Jarvis lab at the University of Wyoming. Owing to the age of the virus it was decided to first characterize the virus by performing immunolabeling to assess the overexpression of CuZnSOD and then using PCR to determine if the viral CuZnSOD homolog gene was properly deleted.

Immunolabeling

Sf-21 cells at a density of 1.5×10^6 cell/mL were infected with Wt AcMNPV, CHC or czSOD virus types at an MOI of 10. At 40 hpi samples were collected. These samples were fixed with 4% paraformalin solution in phosphate buffer solution (PBS) for 15 min at room

temperature. These samples were then cytospined on glass slides at 200 g and permiabilized using 0.1% Tritonx-100 in PBS for 15 min at room temperature. Nonspecific blocking was performed by overlaying slides with normal goat serum (1:400 in PBS) (University of Iowa, central microscopy facility) for 4 h at room temperature. Then the cells were washed with PBS three times (with time 10 min time interval between each wash). Primary antibody rabbit monoclonal to Human CuZnSOD (Dr. Spitz lab, in University of Iowa) was added at 1:400 in PBS for 1 h. Subsequently, the cells were again washed with PBS three times and treated with a secondary antibody conjugated with a fluorescent probe, i.e., Goat Anti Rabbit Alexa 488 (University of Iowa, Central Microscopy Facility). The resulting glass slides were incubated overnight at 4 ^{0}C. The cells were again washed with PBS three times and mounted using vector shield DAPI mounting media (University of Iowa, Central Microscopy Facility) for nuclear staining and mitochondrial staining with Mito tracker Deep Red dye (Invitrogen, Molecular Probes). Zeiss 710 confocal microscope at 40x magnification was used to view and obtain the photographed images.

PCR

A set of primers (5'- TTCTTGCACGCGGCCTTCGC-3' as forward primer and 5'-AACCGGCAATTCTGGCGGCCG-3' as reverse primer) were designed to amplify an approximately 1 kbp segment at the CuZnSOD homolog region (CuZnSOD homolog gene length ~500 bp) of the 134 kbp baculovirus DNA. Another set of primers (5'-GCGCTTTACGCTGCTCCGCGGCGGC -3' as a forward primer and 5'-CTCTTACCGTTATAGGGAAGG -3' as a reverse primer) was used to amplify approximately 1.54 kbp segment at the fp25k region this was used as a control PCR reaction to ensure

DNA presence. The DNA isolation was performed using sucrose gradient method, the protocol for this was obtained from Dr. Robert Harrison (USDA). This protocol is given in Appendix A. Each PCR mixture contained genomic DNA isolated from the budded viruses. Reactions were performed under standard conditions with the Taq DNA polymerase (Roche) in a thermal cycler (Tgradient by Biometra) with the following conditions: 34 cycles of 95 ^{0}C for 1 min, 47 ^{0}C for 45 s, 72 ^{0}C for 1 min, followed by a final cycle of 72 ^{0}C for 7 min. The PCR fragments corresponding to the CuZnSOD homolog region were then purified (Qiagen kit) and sequenced (University of Iowa, DNA Sequencing Facility)

Assays:

Experiments were performed using Sf-21 cells. Cells at a density of 1.5×10^6 cell/mL with a working volume of 40 mL in 250 mL Erlenmeyer flasks were infected with Wt AcMNPV, CHC and czSOD virus types at an MOI of 10. Samples were collected every 24 h and centrifuged at 1000 g for 5 min. Cell pellets were then collected and washed two times with 0.05 M Potassium phosphate saline buffered at 7.8 pH and then stored at -80 ^{0}C. Cell density and viability were also measured using the trypan blue exclusion method using a hemacytometer (Nikon, Melville, NY).

Pellets were thawed and sample preps for SOD, lipid hydroperoxide and protein carbonyl assay were carried out. Samples for SOD assay were prepared by resuspending the pellets in 500 μL DETAPAC buffer at pH 7.8. They were then sonicated on ice twice for 5 s using a Microson ultrasonic cell disruptor (Misonix, Farmingdale, NY) at ~20% full power. Samples for lipid hydroperoxide and protein carbonyl were prepared by resuspending the pellet in PBS solution. The thawed pellet was then lysed twice for 5 s using a sonicator

27

(Misonix, Farmingdale, NY) operated at ~20% full power. Centrifugation at 3000 g for 5 min at 4 ^{0}C for performed to obtain cell homogenate for lipid hydroperoxide assay, whereas for protein carbonyl assay centrifugation was done at 16000 g for 5 min at room temperature. The total protein concentration present in the sample was determined by using the Bradford assay (Bio-Rad Laboratories, Hercules, California, USA). A standard protein curve (0.2–0.9 mg/mL) was prepared using different dilutions of Bovine Serum Albumin (BSA) (Sigma-Aldrich, St. Louis, MO) in ddH$_2$O. The samples were mixed with the reagent dye solution and the absorbance measured at 595 nm.

SOD Assay

The SOD assay was performed as described by Spitz and Oberley (1989) and by using SOD assay kit (Dojindo Molecular Technologies) to determine the of CuZnSOD activity in the cells. SOD levels were measured by determining the inhibition of the change in color of nitroblue tetrazolium or WST-1 (water soluble tetrazolium-1). When converted to formazan caused by the superoxide anion produced using xanthine and xanthine oxidase. SOD standard assay was performed for each sample using 800 μL reaction solution, 100 μL sample in potassium phosphate buffer (pH 7.8) with 0, 2, 4, 10, 25, 100, and 200 μg of total protein, and 100 μL of xanthine oxidase in phosphate buffer. Xanthine oxidase was used at a concentration to produce a color change between 0.016 and 0.023 Abs/min at 560 nm. Absorbance was measured using a UV/VIS spectrophotometer (Thermo scientific, Waltham, MA). To measure total SOD activity levels, the reagents were mixed in a 1 mL cuvette and the absorbance measured every 15 s for 2.5 min at 560 nm. In addition, blanks were run periodically using buffer instead of sample to measure the maximum rate of

28

change obtainable. The rates were recorded for each dilution of each sample. The SOD kit assay used a 96 well plate with 20 µL of sample with 0, 2, 4, 10, 25, 100, and 200 µg of total protein loaded in each well. WST working solution of 200 µL was added to each well. Absorbance was measured at 460 nm after 20 min. The first step in determining CuZnSOD activity involved evaluating the MnSOD activity by adding NaCN to the solution 45 min prior to sample analysis for standard assay and 20 min prior for SOD kit assay to inhibit CuZnSOD. The absorbance rate was measured using the same method as before. After running all samples, the percent inhibition was calculated using Equation 16.

$$\%inhibition = \frac{R_{sod} - R_{blank}}{R_{blank}} \times 100 \qquad (16)$$

Where,

R_{sod} is the rate of change of absorbance of each sample

R_{blank} is the rate of change of absorbance of the blank

Percent inhibition was then plotted against protein concentration. A fitted curve was drawn taking into account all the data points. The protein concentration corresponding to half of the maximum inhibition for all samples was recorded. This concentration depicts one unit activity (U) of the protein in the sample per µg protein concentration which were converted to per mg protein concentration by multiplying with 1000. The level of CuZnSOD activity was determined by calculating the difference between total SOD activity and MnSOD activity.

29

Protein Carbonyl Assay

The principle that reactive oxygen species attack amino acid residues in proteins (especially histidines, arginines, lysines, and prolines) to produce carbonyl products (Levine *et al.,* 1990; Wang *et al.,* 2001) was used to assay protein carbonyl levels. These carbonyl products can be reacted with 2,4-dinitrophenylhydrazine (DNP) (Sigma- Aldrich, St. Louis, MO) to form hydrazone derivatives that can be measured spectroscopically. This assay was conducted by reacting 250 µL of cell homogenate supernatant containing approximately 1 mg/mL of protein with 250 µL of DNP in 2 M HCl (+DNP) at room temperature for 15 min with vortexing every 5 min (Hawkins *et al.*, 2009). After reacting for 15 min, 125 µL 50% trichloroacetic acid was added to the samples and then incubated at -20 ^{0}C for 15 min. Subsequently samples were centrifuged at 9,000 g for 15 min at room temperature. The protein pellet was washed 3 times with ethanol: ethyl acetate (1:1) by centrifuging at 9000 g for 2 min between the washes to remove any leftover reagent without disturbing the pellet. The resulting protein pellet was dissolved in 1 mL of 6 M guanidine-HCl solution. The samples were centrifuged at 9000 g for 2 min to remove any insoluble components. The absorption of the samples treated with DNP (+DNP) was measured at 370 nm and the carbonyl content was determined by using a molar absorption coefficient of 22000 M^{-1}cm^{-1}. 6 M Guanidine-HCl solution was used as the blank. The total protein concentration present in the sample was measured from the samples treated with HCL (-DNP). A calibration curve was prepared by plotting the absorbance of different concentrations of BSA (0-1 mg/mL) in guanidine-HCl at 280 nm from which the sample's final protein concentration was determined. The final protein carbonyl concentration was expressed as

the ratio of the number of moles of carbonyls present in the sample to the protein mass in the sample.

Lipid Peroxidation Assay

Lipid hydroperoxide assay was performed using the BIOXYTECH® LPO-586 assay kit (OXIS International Inc., Beverly Hills, CA). This assay is based on the reaction between malondialdehyde (MDA) and 4-hydroxyalkenals (HAE) (produced due to the decomposition of unstable lipid peroxides) with N-methyl-2-phenylindole in the presence of a methanesulfonic acid. The product is then quantified by determining absorbance at 586 nm. A peroxide calibration plot was developed using the absorbance of different peroxide concentrations at 586 nm by using the standard solution from the manufacturer. This calibration curve was used to determine the peroxide concentration present in the sample. The final lipid hydroperoxide concentration was expressed as the ratio of the number of moles of peroxides in the sample to the mass of the protein present in the sample.

CHAPTER 4 - RESULTS AND DISCUSSION

Effects of Infection caused by modified virus:

Preliminary experiments were performed to determine cell density, cell viability and levels of active CuZnSOD concentration for samples collected at 24, 48, 72 and 96 hpi. There was no significant difference between cell density observed with cells infected with wild type AcMNPV and any of the modified viruses as shown in Figure 8. The modified CHC virus did show higher cell density but the difference was not statistically significant (p> 0.05). Cell density was determined for n = 4. (Where, n is the number of experiments).

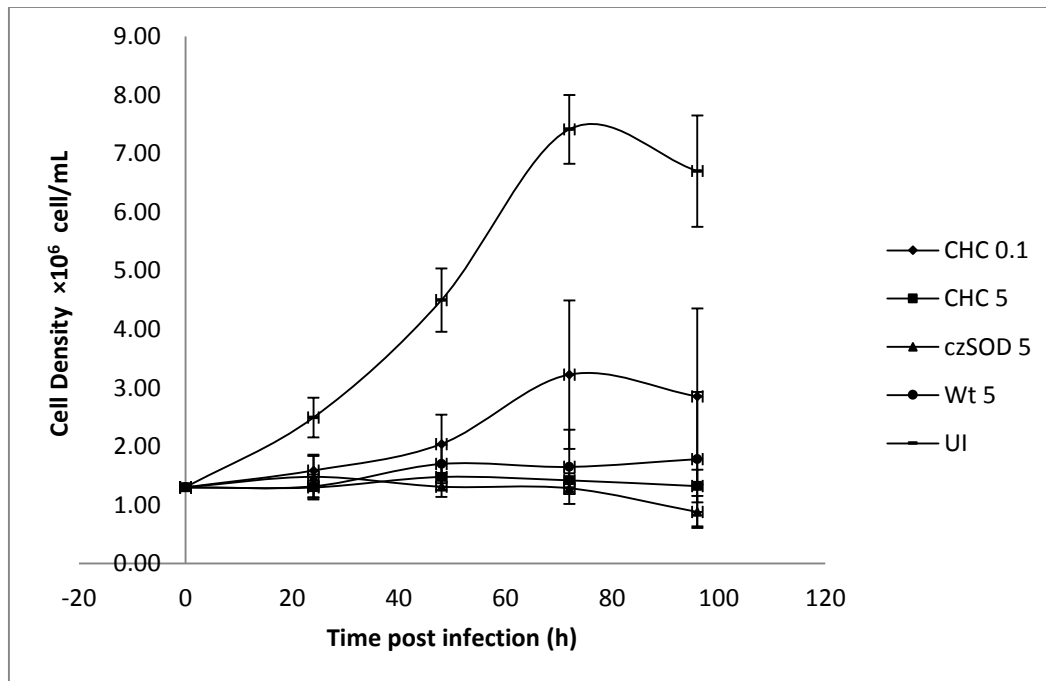**Figure 8: Cell Density of Sf-21 cells infected with different viruses post-infection. The numbers indicated in the series legend corresponds to the MOI of experiment. Error bars represent 95% confidence levels (n=4).**

The uninfected cells show the highest cell viability followed by the CHC virus with different MOI's, whereas the czSOD virus showed lowest cell viability after 96 hpi but fail

to show a statistically significant difference ($p > 0.05$) in the viability of cells infected with different modified viruses. The cell viability plots shown are in Figure 9.

Figure 9: Cell viability of Sf-21 cells infected with different viruses post-infection. The numbers indicated in the series legend corresponds to the MOI of experiment. Error bars represent 95% confidence levels (n=4).

CuZnSOD activity in the cells infected with the modified viruses are shown in Figure 10. It was expected CHC virus would have a significantly higher activity compared to the wild type and czSOD viruses. The CuZnSOD activity levels would be expected to remain constant and be greater than in cells infected with the Wt-AcMNPV virus. But the results depicted in Figure 10 showed a high variability and did not follow any particular pattern. As a result it was suggested that virus should be characterized to determine that the correct modifications were performed.
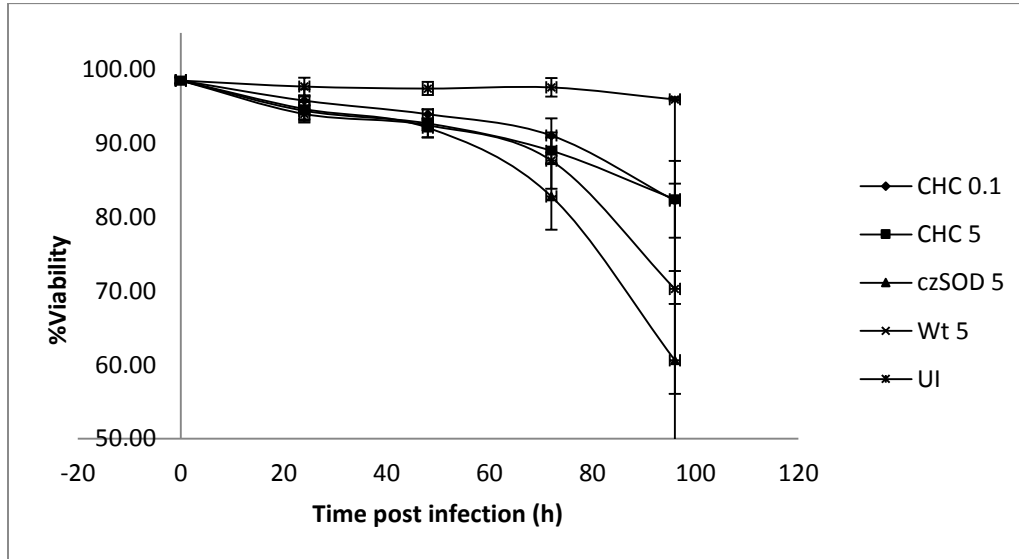
33
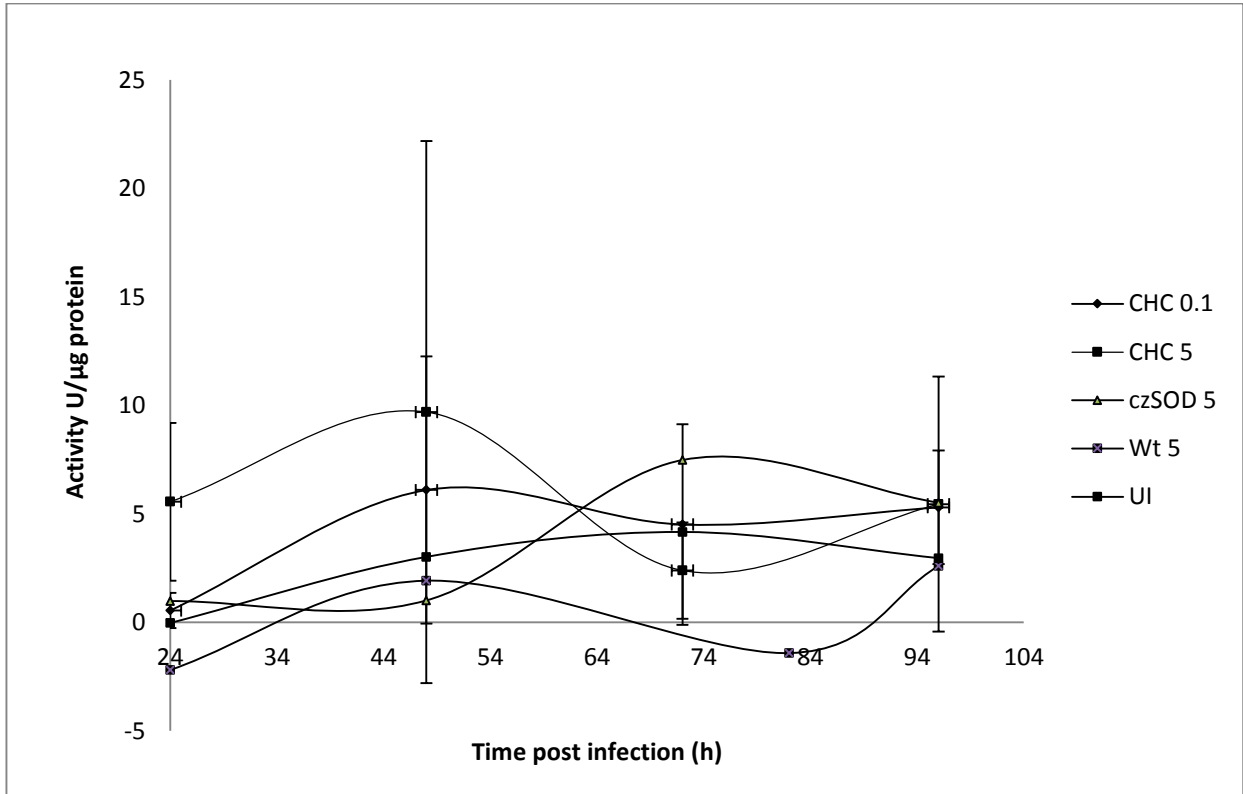
Figure 10: CuZnSOD activity in Sf-21 cells infected with different viruses post-infection. The numbers indicated in the series legend corresponds to the MOI of experiment. Error bars represent 95% confidence levels (n=4).

Information on modified virus obtained from characterization:

The immunofluorescence assay was performed using the following virus types: Wt-AcMNPV, czSOD virus and CHC virus (see Table 1). It can be seen from Figure 11 that both the modified viruses showed overexpression of CuZnSOD in the cells, whereas the Wt and the uninfected cells showed relatively lower expression as predicted.

34
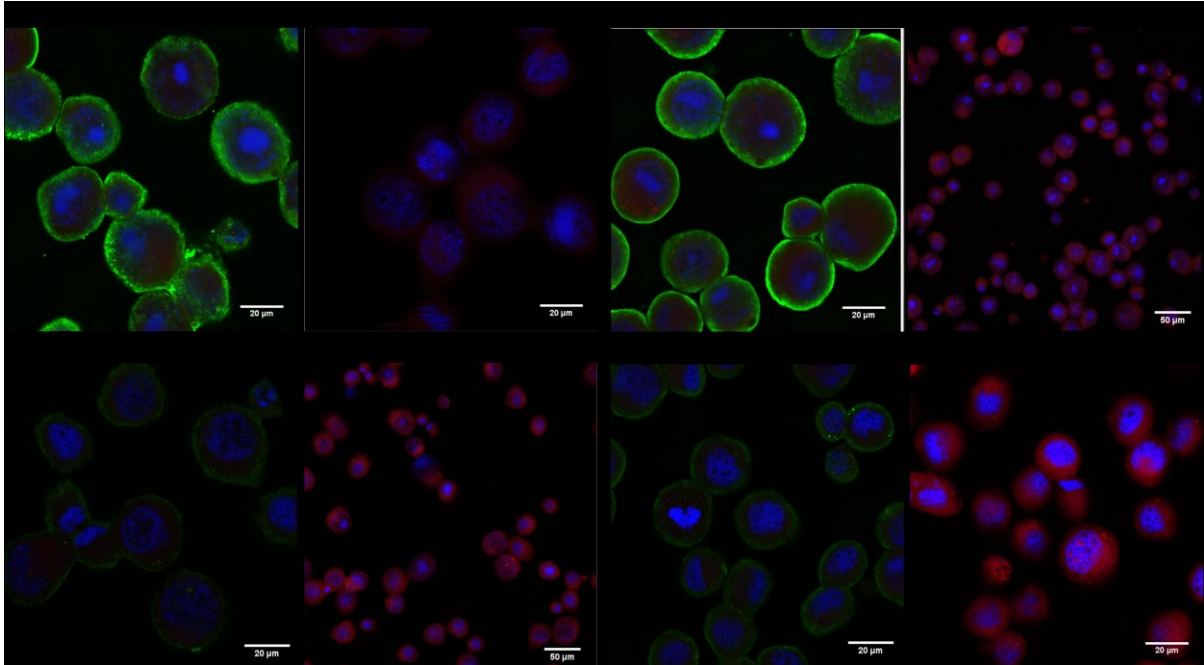
Figure 11: Confocal microscopy of cells infected with modified viruses shows that CuZnSOD is overexpressed in czSOD and CHC- infected cells and not in cells infected with Wt-AcMNPV or in uninfected cells(at 40 hpi). The expression of human CuZnSOD protein in single cells was determined using a double labeling technique. The infected cells were stained with antibody against human CuznSOD (green stain indicating human CuZnSOD expression), mitochondria (red stain) and nuclei (blue stain).

Genetic analysis using PCR was performed on Wt-AcMNPV, czSOD, CHC and AvSOD viruses (see Table 1) to determine the exact deletion or disruption of the viral CuZnSOD homolog gene in the modified viruses. The presence of the CuZnSOD homolog gene was shown by formation of the corresponding 1 kb product obtained in the baculovirus DNA. Wt-AcMNPV was used as a positive control for this reaction. From Figure 12 it can be seen that the czSOD virus DNA contained the viral CuZnSOD homolog as predicted and that the AvSOD virus showed a small amount of PCR product formation of different lengths depicting that the CuZnSOD homolog gene was disrupted. The CHC virus, which was expected to have a complete deletion of this region, showed a product formed with 85%

35

sequence match to the CuZnSOD homolog gene. This showed that the CHC virus was not a

pure modified virus, i.e., that it contained the CuZnSOD homolog gene. This explained the

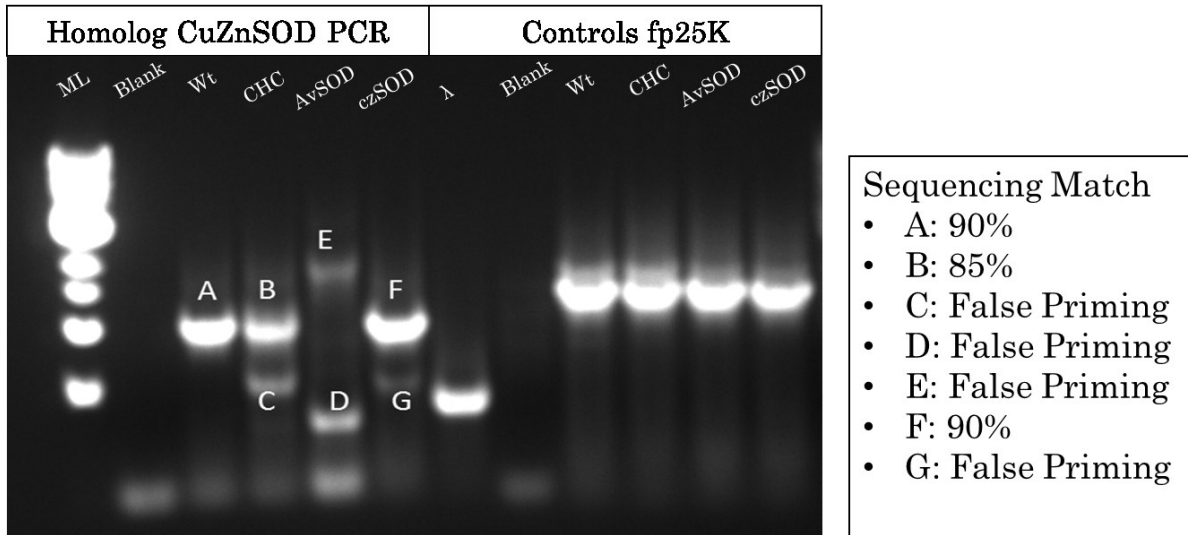discrepancy seen in the previous cell viability and cell density data.

Figure 12: PCR product obtained for viral homolog CuZnSOD gene and control fp25k gene.

Effects of induced oxidative stress:

Effects of induced oxidative stress were studied by introducing H_2O_2 as an oxidative

stress inducer and it can be seen from the Figure 13 that the viral infection was enhanced

in the presence of oxidative stress.

<div align="center">

cells + virus + H₂O₂ (same   cells + virus + H₂O₂ (same   cells + H₂O₂ + (Virus 1 h later)   cells + virus (No H₂O₂) 72 h pi   uninfected cells control
time) 48 h pi   time) 72 h pi   72 h pi

</div>
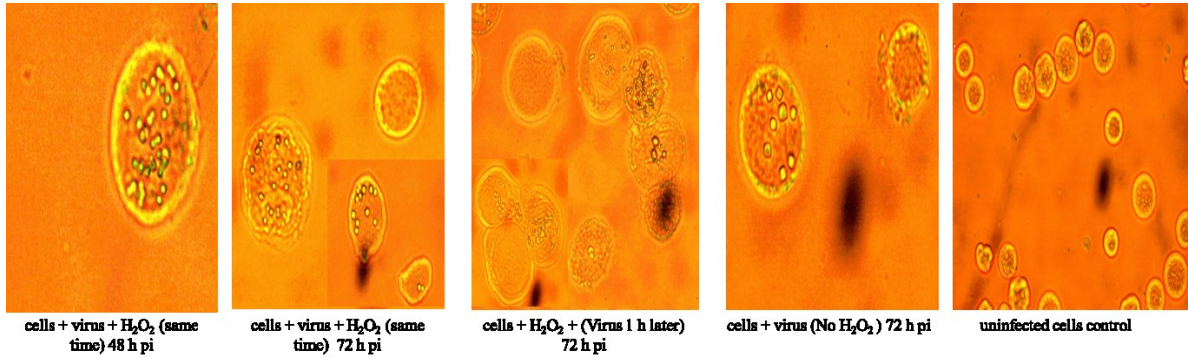
Figure 13: Various stages of polyhedra formation as indication of enhanced infectivity due to induced oxidative stress.

The faulty modified virus was redeveloped by Dr. Christoph Geisler, University of Wyoming. As it was previously observed that some oxidative stress was required for normal infection, the new virus was titered in presence of 10 µM H_2O_2 and it was found as summarized from Table 2 that this resulted in higher infectivity.

Table 2: Effect of induced oxidative stress on viral infection

Type of Virus	Virus Titer	
	With 10µM H_2O_2	Without H_2O_2
CHCpp1	1×10^{10} pfu/mL	1.3×10^8 pfu/mL
Wt-AcMNPV	4.14×10^8 pfu/mL	1.7×10^8 pfu/mL

Cell density, viability and CuZnSOD activity assays done without the new CHCpp1 virus showed that just overexpressing human CuZnSOD or viral modification with just the homolog CuZnSOD gene disruption, did not increase or maintain the CuZnSOD activity in the cells post-infection.

37

Figure 14: Cell density of Sf-21 cells infected with different viruses post-infection (MOI 10). Error bars represent 95% confidence levels (n=3).

Cell densities for infected cells remained nearly constant after infection compared to the uninfected cells. The AvSOD infection analysis was not conducted in the preliminary experiments. And it could be seen that the modification to disrupt viral CuZnSOD homolog did not show any statistically significant effect (p> 0.05) on the cell density or cell viability of the infected cells (Figure 14 and 15).

38

Figure 15: Cell viability of Sf-21 cells infected with different viruses post-infection (MOI 10). Error bars represent 95% confidence levels (n=3).

The CuZnSOD activity levels also reduced to 0 after 72 hpi as seen in Figure 16. As the CuZnSOD activity is calculated by taking the difference between the total SOD and the MnSOD activity in the cell, the negative values indicate the absence of CuZnSOD activity i.e., 0 U/µg activity. The czSOD virus shows a marginal difference in time for the CuZnSOD activity to drop to zero compared to the Wt-AcMNPV.
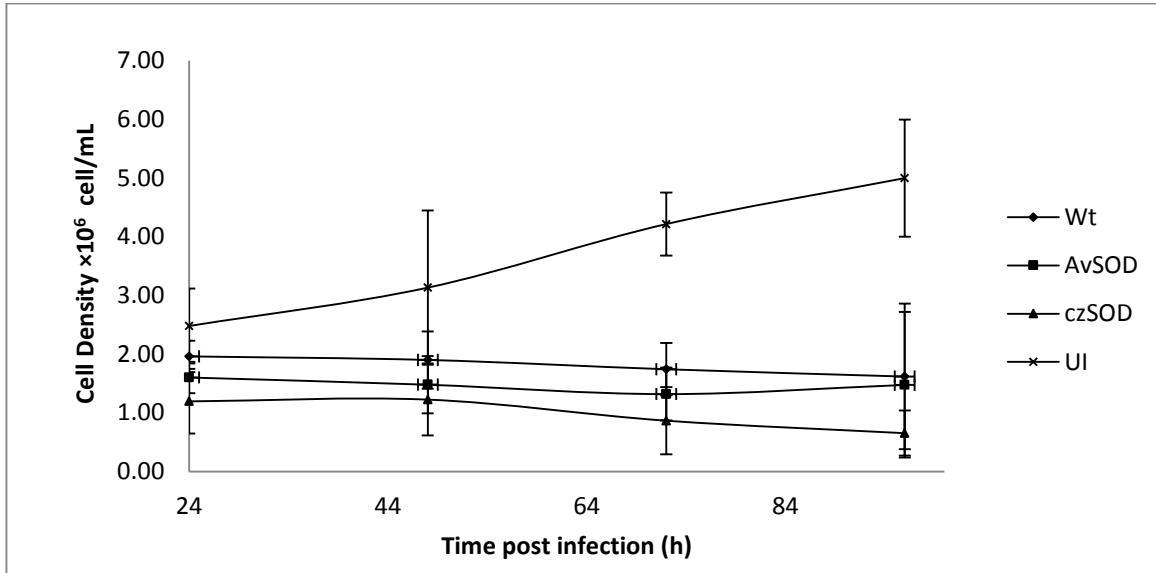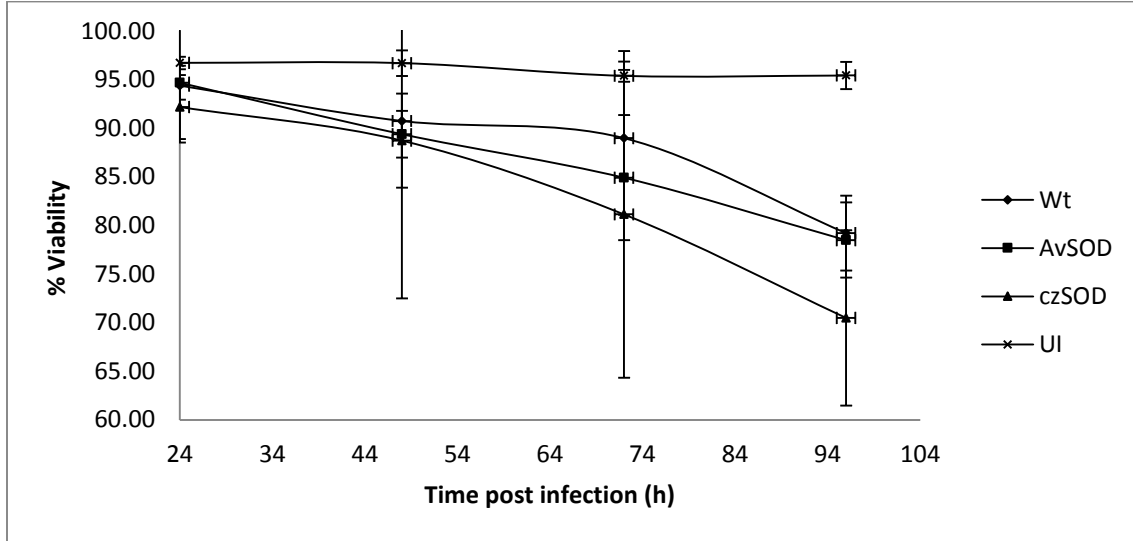
39
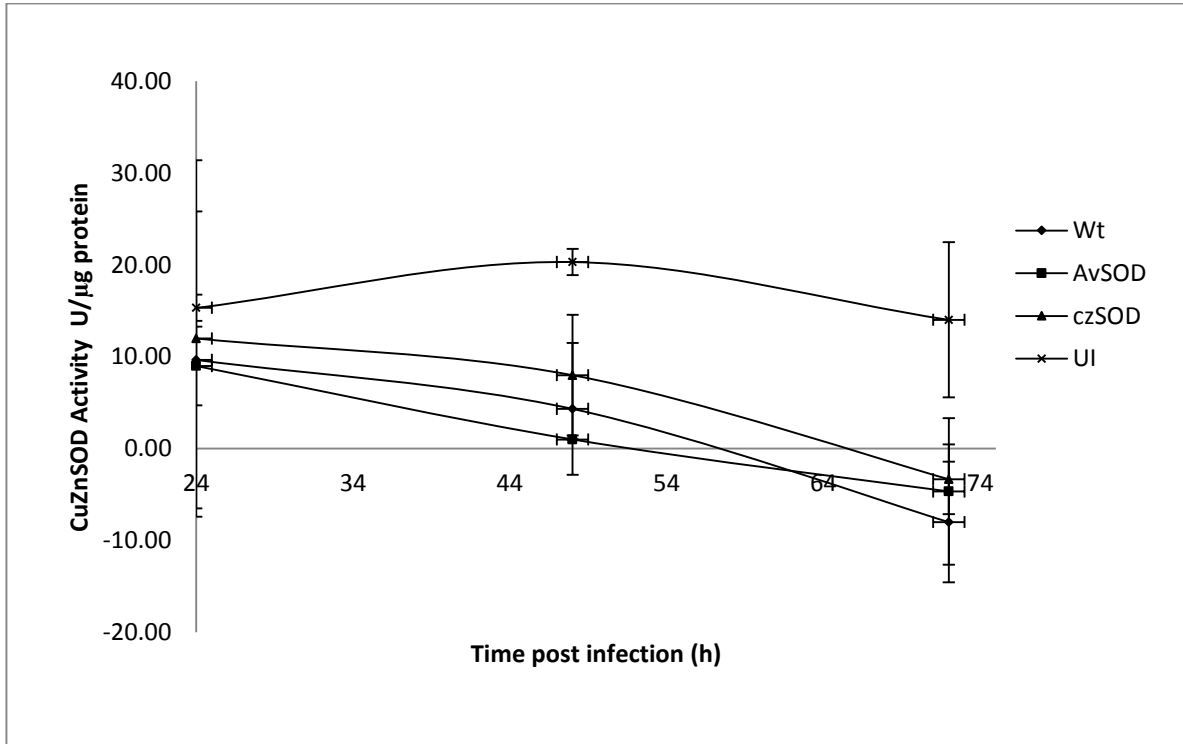
Figure 16: Activity of CuZnSOD in Sf-21 cells infected with different viruses post-infection (MOI 10). Error bars represent 95% confidence levels (n=3).

The fall in cell viability post 40 hpi and the decreasing CuZnSOD activity during the same time indicate that maintaining CuZnSOD activity is important for the maintaining cell viability. Further experiments using the CHCpp1 virus with overexpression of human CuZnSOD/CCS and deletion of the viral CuZnSOD homolog showed that increased CuZnSOD activity correlated with increased cell viability post-infection.

The final experiment set (n = 3) included CHCpp1 virus in addition to the previous set, Wt- AcMNPV virus, czSOD virus and AvSOD virus(see Table 1 and Figures 17 and 18). The cell density and cell viability were compared for all the types of viruses. The uninfected cells showed increase in cell density with time as expected, whereas the infected cells remained nearly at a constant cell density.
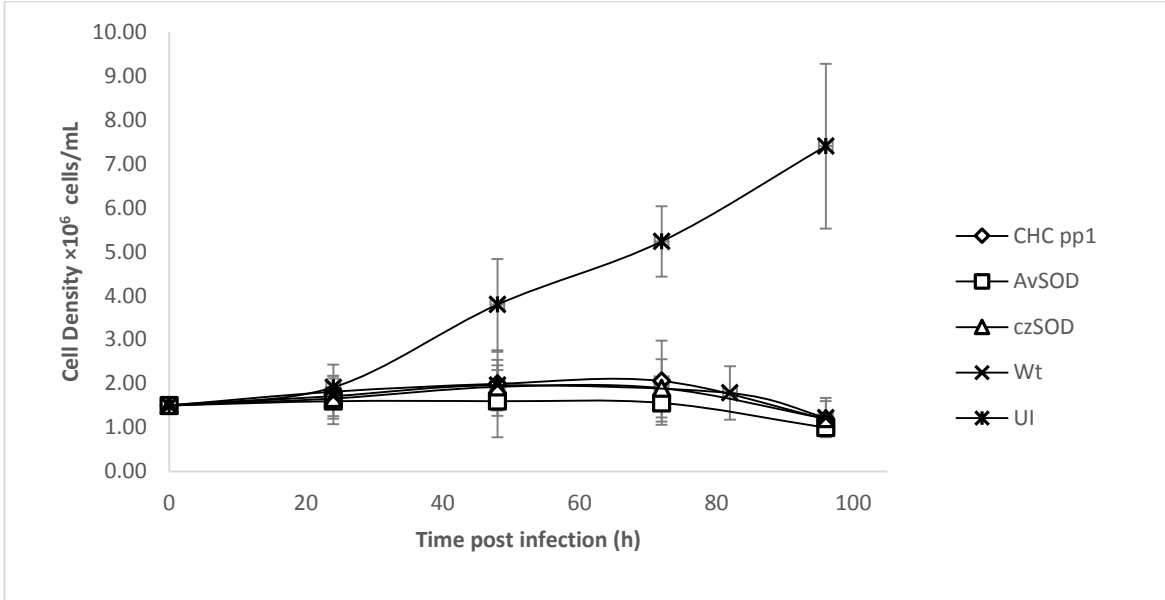
Figure 17: Cell density of Sf-21 cells post-infection for the final experiment set (MOI 10). Error bars represent 95% confidence levels (n=3).

As expected after viral infection the cell growth is restricted and the decrease in the cell density 60 hpi is indicative of cell death. The cell viability for CHCpp1 virus is higher compared to the all the other modified viruses as well as Wt-AcMNPV but is not significantly higher (p> 0.05), as shown in Figure 18. This suggests that reduction in oxidative stress might give cells a prolonged life.

41
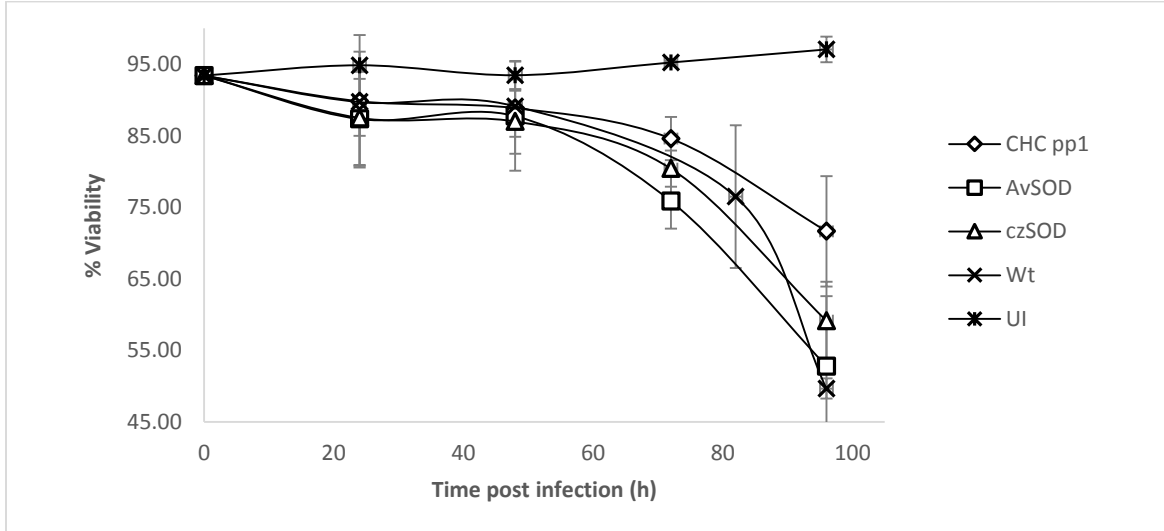
Figure 18: Cell viability of Sf-21 cells post-infection for the final experiment set (MOI 10). Error bars represent 95% confidence levels (n=3).

CuZnSOD assay was performed to determine the CuZnSOD activity. As projected CHCpp1 showed higher levels of CuZnSOD activity compared to all other virus types as shown in Figure 19. This also validates the higher cell viability seen for this virus-post infection. The negative CuZnSOD activity seen in czSOD and Wt-AcMNPV virus after ~60 hpi and 48 hpi respectively indicates that there is no active CuZnSOD present in the cells. The CHCpp1 virus shows significantly higher CuZnSOD activity ($p > 0.05$) in the cells 100 hpi compared to the Wt-AcMNPV and other modified viruses.

42

Figure 19: CuZnSOD activity in Sf-21 cells infected with different viruses post-infection for the final experiment set (MOI 10). Error bars represent 95% confidence level (n=3). (B) Plotted without the AvSOD virus to show an improved scale for other viruses.

Lipid peroxide formation is an indication of increased oxidative stress. Uninfected cell samples were run as the negative control and, as expected, had the least amount of lipid peroxides. The lipid peroxide formation in cells infected with Wt-AcMNPV, czSOD and AvSOD showed maximum lipid peroxide concentrations at 72 hpi as shown in Figure 20. The difference of lipid peroxide concentration in the CHCpp1 compared to Wt-AcMNPV and other modified viruses was significantly lower (p> 0.05).

Figure 20: Lipid hydroperoxide concentrations in Sf-21 cells infected with different viruses post-infection for final experiment set (MOI 10). Error bars represent 95% confidence levels (n=3).

Protein Carbonyl formation results from protein oxidation and can also be used as an oxidative stress marker. Figure 21 shows the concentration of protein carbonyls as a function of time post-infection. This assay was not conclusive due to high deviations. But the Wt-AcMNPV did show higher protein carbonyls present at 100 hpi and it had the least viability (see Figure 18). Protein carbonyl levels are lower for CHCpp1 virus and uninfected cells compared to the other modified viruses as seen in Figure 21-B but the values are not statistically significant (p> 0.05) due to high deviations.
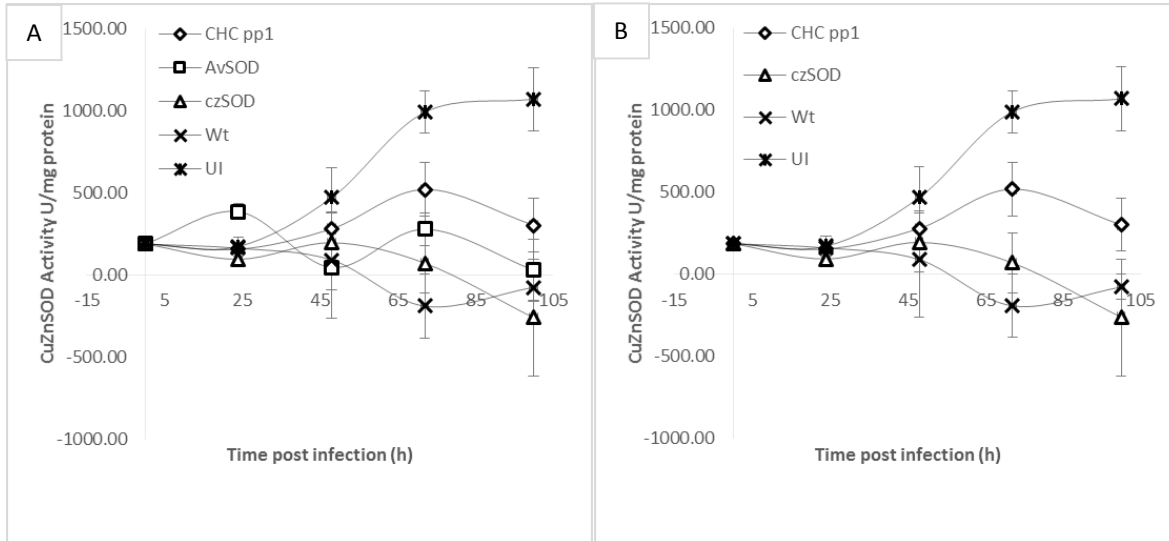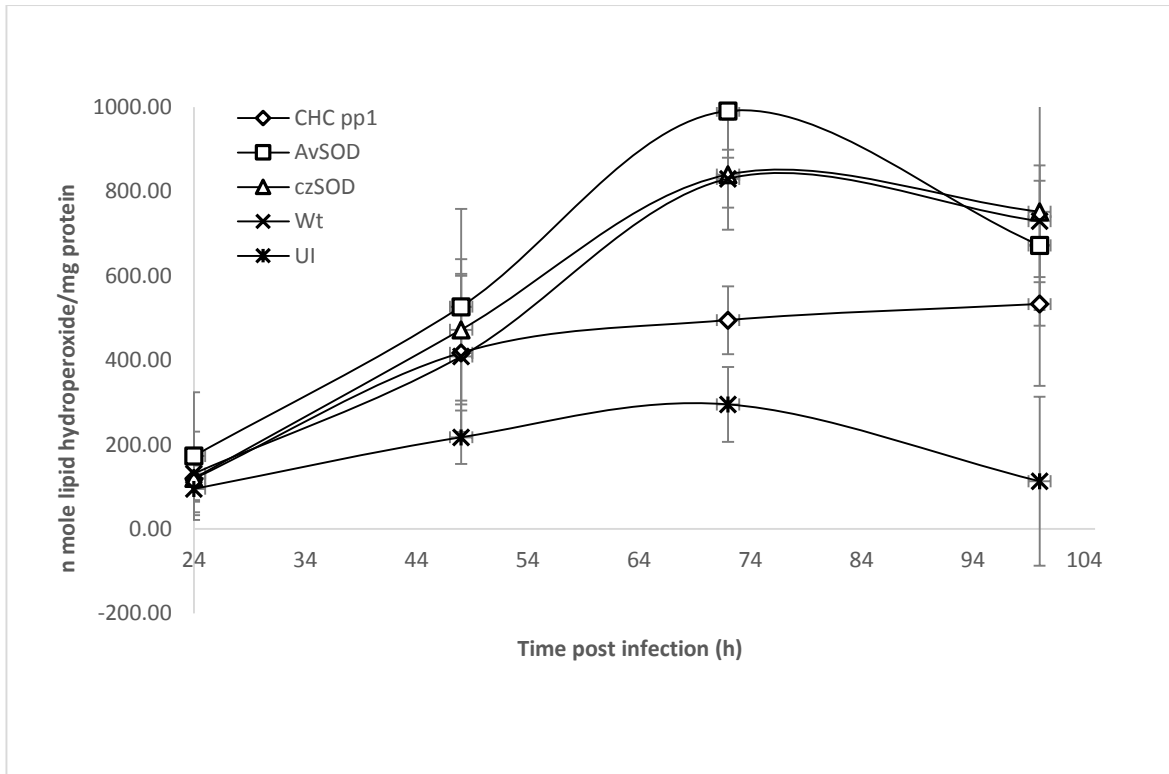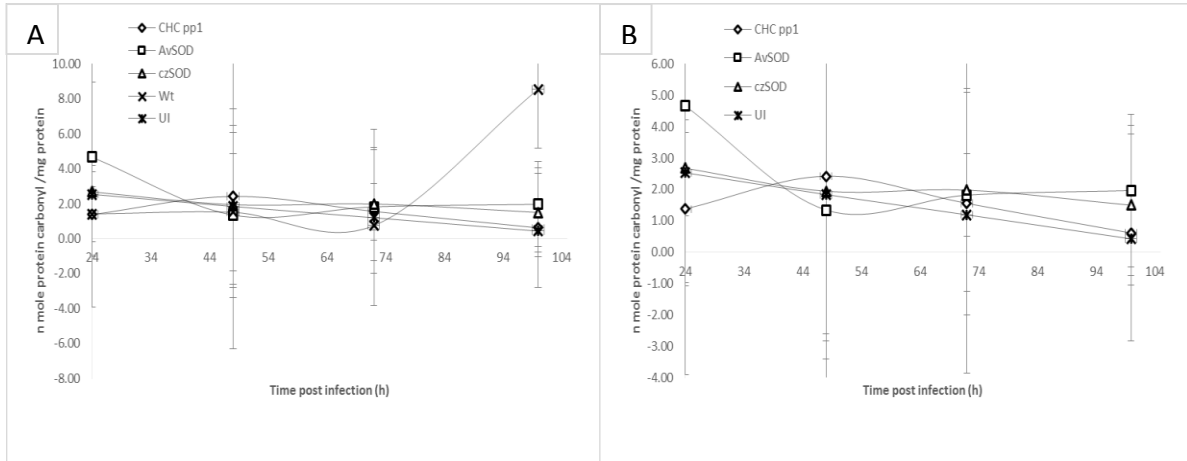
44

Figure 21: Protein Carbonyl concentrations in Sf-21 cells infected with different viruses post-infection for the final experiment set (MOI 10). Error bars represent 95% confidence levels (n=3). (B) Plotted without the Wt-AcMNPV to show an improved scale for other modified viruses.

CHAPTER 5 - CONCLUSION AND FUTURE WORK

It was demonstrated that the CuZnSOD homolog coded by the AcMNPV genome eliminated CuZnSOD activity, thereby causing increased oxidative stress. The cells infected with AvSOD and czSOD viruses showed a decrease in CuZnSOD activity by 40-60 hpi. The cells infected with modified virus CHCpp1 show higher CuZnSOD activity and cell viability, and lower lipid peroxide and protein carbonyl concentrations, thereby demonstrating that increased oxidative stress can lead to cell death. The viability of cells after 40-60 hpi rapidly decreased and was indicative that CuZnSOD activity is important for cells to combat the higher oxidative stress caused by viral infection and that the lack of this enzyme leads to cell death under these conditions.

Future investigations should be conducted to determine the mechanism responsible for the binding of the viral CuZnSOD homolog to the CuZnSOD chaperone to shed some light into why the virus requires a SOD protein decoy mechanism. Since oxidative stress has been shown to increase cell death, further modification of the CHCpp1 virus should be done to include the expression of valuable recombinant proteins. Specifically, its protein yield over time can be tested in comparison to the more traditionally used techniques. This will improve the understanding of the effects of reducing oxidative stress in cells post-infection that may result in an improved BEVS.

APPENDIX A

ISOLATION OF BACULOVIRUS DNA FROM BUDDED VIRUS

1) Centrifuge infected cell medium at approx. 1000 g for 5 min to pellet detached cells and polyhedra.

2) Transfer up to 33 mL supernatant each to SW28 ultracentrifuge tubes.

3) Layer 3 mL of 25% w/w sucrose in PBS underneath the infected cell medium.

- "25% w/w" means that for each 100 g solution, 25 g is sucrose. Prepare as much fresh sucrose solution as needed for each iteration of this method – do not use old sucrose solution. Use a pipette pump (plastic thing with a thumb wheel) and bring the pipette tip down to the bottom of the SW28 tube, then slowly pipette the sucrose solution to form the sucrose pad through which BV will be centrifuged. Balance tubes with PBS.

4) Pellet BV by centrifugation in an SW28 rotor, 103586 g for 75 min.

5) Pour off supernatant and re-suspend pellets in 500 μL disruption buffer (10 mM Tris-HCl pH 8.0, 10 mM EDTA pH 8.0, 0.25% SDS), 2 pellets/500 μL buffer. Add proteinase K to a final concentration of 500 g/mL.

- Wash SW28 buckets – if they have sucrose on/in them, wash them ASAP. Use the green Beckman SSS rotor detergent and a Beckman rotor brush, and replace black rubber O-rings that come out of the buckets (these usually get tangled up in the rotor brush).

6) Incubate fully re-suspended pellets at 37 °C for 3 hr (or more for big pellets that produce very viscous suspensions). If necessary, the DNA can be allowed to incubate overnight.

7) Extract pellets once with phenol, once with 1:1 phenol:chloroform, and once with chloroform. Mix by inversion, not vortexing.

8) Ethanol-precipitate DNA as usual (2x volume 95 – 100% ethanol, 1/10x volume 3 M NaOAc pH5.2).

9) Pellet by microcentrifugation, re-suspend in a minimum volume of dH_2O.

SAMPLE VIRUS TITER CALCULATION

Table B-1: Establishing virus titer using Excel spreadsheet for end point dilution assay.

Dilutions	Number of Infected Wells	Number of Uninfected Wells	Total Number Infected	Total Number Uninfected	% Total Infected	Above 0.5	Number of Infected Wells	Number of Uninfected Wells	Log Dilution Above 50%
1.00E-03	12	0	72	0	1	TRUE	0	0	0
1.00E-04	12	0	60	0	1	TRUE	0	0	0
1.00E-05	12	0	48	0	1	TRUE	0	0	0
1.00E-06	12	0	36	0	1	TRUE	0	0	0
1.00E-07	12	0	24	0	1	TRUE	0	0	0
1.00E-08	7	5	12	5	0.705882353	TRUE	0.705882353	0	-8
1.00E-09	5	7	5	12	0.294117647	FALSE	0	0.294117647	0
1.00E-10	0	12	0	24	0	FALSE	0	0	0
Num. Wells	12						0.705882353	0.294117647	-8
mL/well	0.02								
Prop. Dist.	0.5								
Log TCID	-8.5								
TCID50	3.16228E-09								
1/TCID50	316227766								
TCID50/ml	15811388301								
pfu/ml	10909857928								

EXPERIMENTAL DATA

Table C-1: CuZnSOD activity for experiment set without CHCpp1 virus.

Virus Type	MOI	Time post infection (h)	CuZnSOD Activity U/mg			Mean	Std. deviation	95% confidence
Wt	10	24	3000	10000	16000	9666.667	6506.407	16162.811
	10	48	1000	6000	6000	4333.333	2886.751	7171.0879
	10	72	-11000	-6000	-7000	-8000	2645.751	6572.4106
AvSOD	10	24	10000	7000	10000	9000	1732.051	4302.6527
	10	48	1000	1000	1000	1000	0	0
	10	72	-7000	-6000	-1000	-4666.67	3214.55	7985.3855
CuZnSOD	10	24	16000	17000	3000	12000	7810.25	19401.736
	10	48	5000	9000	10000	8000	2645.751	6572.4106
	10	72	-5000	-2000	-3000	-3333.33	1527.525	3794.583
UI	10	24	16000	15000	15000	15333.33	577.3503	1434.2176
	10	48	21000	20000	20000	20333.33	577.3503	1434.2176
	10	72	10100	16000	16000	14033.33	3406.367	8461.8837

Table C-2: Cell density and cell viability data after infection for experiments without the CHCpp1 virus.

Virus Type	MOI	Time post infection hr	Cell Density ×10^6 cells/mL			Viability			Mean Cell Density ×10^6 cells/mL	Mean Viability	95% confidence	Std Dev. Cell Density ×10^6 cells/mL	Std Dev. Viability	95% confidence
Wt	10	24	1.99	2.2	1.69	94.76	96.5	91.84	1.96	94.37	0.64	0.26	2.35	5.85
	10	48	2.1	2.3	1.3	95.45	94.48	82.27	1.90	90.73	1.31	0.53	7.35	18.25
	10	72	1.82	1.91	1.5	92.38	88.42	86.11	1.74	88.97	0.54	0.22	3.17	7.88
	10	96	1.8	1.9	1.16	78.9	80.9	77.85	1.62	79.22	1.00	0.40	1.55	3.85
AvSOD	10	24	1.65	1.48	1.68	94.18	95.48	94.38	1.60	94.68	0.27	0.11	0.70	1.74
	10	48	1.7	1.42	1.32	88.54	90.44	89.18	1.48	89.39	0.49	0.20	0.97	2.40
	10	72	1.51	1.3	1.15	87.28	85.3	82.14	1.32	84.91	0.45	0.18	2.59	6.44
	10	96	2.01	1.4	1.02	79.44	79.33	76.69	1.48	78.49	1.24	0.50	1.56	3.87
czSOD	10	24	1.1	1.04	1.45	91.66	93.69	91.19	1.20	92.18	0.55	0.22	1.33	3.30
	10	48	1.19	1	1.49	88.14	90.9	87.13	1.23	88.72	0.61	0.25	1.95	4.85
	10	72	0.77	0.7	1.13	74.03	87.5	81.88	0.87	81.14	0.57	0.23	6.77	16.81
	10	96	0.83	0.59	0.54	68.59	74.68	68.2	0.65	70.49	0.39	0.16	3.63	9.03
UI	10	24	2.78	2.78	1.88	96.86	96.86	96.41	2.48	96.71	1.29	0.52	0.26	0.65
	10	48	3.23	3.23	2.94	96.99	96.99	96.07	3.13	96.68	0.42	0.17	0.53	1.32
	10	72	4.38	4.38	3.89	95.53	95.53	95.11	4.22	95.39	0.70	0.28	0.24	0.60
	10	96	4.96	4.96	5.08	95.75	95.75	94.77	5.00	95.42	0.17	0.07	0.57	1.41

51

Table C-3: Cell Density and cell viability data after infection for the final experiment set.

Virus Type	MOI	Time post infection	Cell Density ×10^6 cells/mL						Viability					
			1	2	3	Avg.	95% C	std. dev	1	2	3	Avg.	95% C	std. dev
CHC pp1	10	0	1.5	1.5	1.5	1.50	0.00	0.00	93.4	93.4	93.4	93.40	0.00	0.00
CHC pp1	10	24	1.53	1.99	1.92	1.81	0.62	0.25	85.95	93.4	90.1	89.82	9.27	3.73
CHC pp1	10	48	1.81	1.84	2.33	1.99	0.73	0.29	87	89.6	89.96	88.85	4.01	1.62
CHC pp1	10	72	2.47	1.75	1.95	2.06	0.92	0.37	85.76	83.33	84.69	84.59	3.03	1.22
CHC pp1	10	96	1.15	1.2	1.22	1.19	0.09	0.04	69.5	70.2	75.2	71.63	7.72	3.11
AvSOD	10	0	1.5	1.5	1.5	1.50	0.00	0.00	93.4	93.4	93.4	93.40	0.00	0.00
AvSOD	10	24	1.39	1.81	1.59	1.60	0.52	0.21	84.75	90.04	87.2	87.33	6.58	2.65
AvSOD	10	48	1.23	1.87	1.69	1.60	0.82	0.33	84.24	90.03	88.94	87.74	7.64	3.08
AvSOD	10	72	1.6	1.73	1.34	1.56	0.49	0.20	74.07	76.88	76.57	75.84	3.83	1.54
AvSOD	10	96	0.98	0.99	1.01	0.99	0.04	0.02	50.8	50.2	57.3	52.77	9.78	3.94
czSOD	10	0	1.5	1.5	1.5	1.50	0.00	0.00	93.4	93.4	93.4	93.40	0.00	0.00
czSOD	10	24	1.73	1.59	1.66	1.66	0.17	0.07	90.5	85.48	86.5	87.49	6.59	2.65
czSOD	10	48	1.85	2.1	1.82	1.92	0.38	0.15	86.04	89.1	85.84	86.99	4.54	1.83
czSOD	10	72	1.72	1.76	2.2	1.89	0.66	0.27	81.22	79.27	80.7	80.40	2.51	1.01
czSOD	10	96	1.3	1.02	1.29	1.20	0.39	0.16	59.01	57.02	61.4	59.14	5.45	2.19
Wt	10	0	1.5	1.5	1.5	1.50	0.00	0.00	93.4	93.4	93.4	93.40	0.00	0.00
Wt	10	24	1.51	1.87	1.77	1.72	0.46	0.19	91.5	89.9	87.7	89.70	4.74	1.91
Wt	10	48	1.93	1.75	2.21	1.96	0.58	0.23	88.9	88.38	90.07	89.12	2.15	0.87
Wt	10	82	1.71	1.59	2.06	1.79	0.61	0.24	80.28	72.27	76.86	76.47	9.98	4.02
Wt	10	96	1.4	1.23	1.04	1.22	0.45	0.18	50.02	49	49.95	49.66	1.42	0.57
UI	0	0	1.5	1.5	1.5	1.50	0.00	0.00	93.4	93.4	93.4	93.40	0.00	0.00
UI	0	24	2.02	1.81	1.92	1.92	0.26	0.11	93.95	95.26	95.3	94.84	1.91	0.77
UI	0	48	3.68	3.45	4.26	3.80	1.04	0.42	94.35	93.18	92.81	93.45	2.00	0.80
UI	0	72	5.1	5.6	5	5.23	0.80	0.32	95.32	95.13	95.23	95.23	0.24	0.10
UI	0	96	7.5	8.1	6.6	7.40	1.88	0.75	97.8	97	96.36	97.05	1.79	0.72

Table C-4: CuZnSOD Activity post infection for the final experiment set.

Virus Type	MOI	Time post infection	CuZnSOD Activity	U/mg protein				
			1	2	3	Avg.	std. dev	95% Confidence
		0	187.61	187.61	187.61	187.61	0.00	
CHC pp1	10	24	241.57	103.18	120.13	154.96	75.48	187.51
	10	48	234.98	205.59	398.97	279.85	104.20	258.86
	10	72	357.8671	684.83	516.04	519.58	163.51	406.18
	10	100	180.00	240.25	484.65	301.63	161.33	400.78
		0	187.61	187.61	187.61	187.61	0.00	
AvSOD	10	24	384.20	338.17	430.99	384.45	46.41	115.30
	10	48	153.64	84.47	-106.46	43.88	134.72	334.66
	10	72	162.045	330.1979	340.05	277.43	100.05	248.53
	10	100	167.38	105.07	-187.91	28.18	189.72	471.28
		0	187.61	187.61	187.61	187.61	0.00	
czSOD	10	24	93.77	75.88	112.60	94.08	18.36	45.61
	10	48	404.07	107.68	72.78	194.84	182.03	452.19
	10	72	-135.781	201.1361	144.61	69.99	180.43	448.21
	10	100	-118.25	0.00	-667.67	-261.97	356.28	885.06
		0	187.61	187.61	187.61	187.61	0.00	
Wt	10	24	139.90	162.49	181.32	161.24	20.74	51.52
	10	48	234.98	348.52	-313.10	90.14	353.79	878.87
	10	72	-190.142	-384.99	0.53	-191.53	192.76	478.85
	10	100	-156.84	-73.05	0.00	-76.63	78.48	194.96
		0	187.61	187.61	187.61	187.61	0.00	
UI	0	24	154.02	125.78	236.49	172.10	57.53	142.91
	0	48	391.26	336.31	679.94	469.17	184.59	458.55
	0	72	850.9651	1096.32	1024.00	990.43	126.08	313.19
	0	100	853.32	1132.56	1223.12	1069.67	192.76	478.83

REFERENCES

Belyaev, A. S.; Hails, R. S.; Roy, P. High-level expression of five foreign genes by a single recombinant baculovirus *Gene.* **1995,** 156, 229-233.

Boveris, A.; and Chance, B. The Mitochondrial Generation of Hydrogen Peroxide *Biochemical Journal*. **1973,** 19, 707-716.

Bradford, M. M. A rapid and sensitive method for the quantitation of microgram quantities of protein utilizing the principle of protein-dye binding *Anal Biochem*. **1976,** 72, 248-54.

Butler, M. Animal cell cultures: recent achievements and perspectives in the production of biopharmaceuticals *Appl. Microbial. Biotechnol*. **2005,** 68:283-291

Cao, J. X.; Teoh M. L. T.; Moon, M.; McFadden, G.; Evans, D. H. Leporipoxvirus Cu-Zn Superoxide Dismutase Homologs Inhibit Cellular Superoxide Dismutase, but Are Not Essential for Virus Replication or Virulence *Virology.* **2002,** 296, 125-135.

Coleman, T. A.; Parmelee, D.; Thotakura, N. R.; Nguyen, N.; Bürgin, M.; Gentz, S.; Gentz, R. Production and purification of novel secreted human proteins *Gene.* **1978,** 190, 163-171.

Federici, B.A. Baculovirus pathogenesis. *In The Baculoviruses*; Miller, L.K., Ed.; Plenum Press: New York, 1997; pp 33-59.

Gotoh T.; Miyazaki Y.; Kikuchi K.-I.; Bentley, W. E. Investigation of sequential behavior of carboxyl protease and cysteine protease activities in virus-infected Sf-9 insect cell culture by inhibition assay *Appl Microbiol Biotechnol.* **2001,** 56, 5-6

Halliwell, B. Superoxide-dependent formation of hydroxyl radicals in the presence of iron salts: Its role in degradation of hyaluronic acid by a superoxidegenerating system *FEBS Letters.* **1978,** 96, 238-242.

Halliwell, B. Free radicals, antioxidants, and human disease: curiosity, cause, or consequence? Lancet **1994,** 344, 721-4.

Halliwell, B.; Gutteridge, J. M. Oxygen toxicity, oxygen radicals, transition metals and disease *Biochem J.* **1984,** 219, 1–14.

Halliwell, B.; Gutteridge, J. Ed*. Free Radicals in Biology and Medicine,* 4th ed. Oxford University Press, USA. 2007; pp 260-264,

Harrison, R. L.; Jarvis, D. L. Transforming Lepidopteran Insect Cells for Improved Protein Processing *In The Biology of Baculoviruses* **2007,** 1, 341-356.

Harrison, R. L.; Jarvis, D. L. Transforming Lepidopteran Insect Cells for Continuous Recombinant Protein Expression *In Baculovirus and Insect Cell Expression Protocols*, 2007; pp 299-315.

Harrison, R. L.; Summers, M. D. Mutations in the Autographa californica multinucleocapsid nuclear polyhedrosis virus 25 kDa protein gene result in reduced virion occlusion, altered intranuclear envelopment and enhanced virus production *J Gen Virol*. **1995,** 76, 1451-1459.

Hawkins, C.L.; Morgan, P.E.; Davies, M. J. Quantification of protein modification by oxidatants *Free Radic. Biol. Med.* **2009**, 46, 965-988

Hughes, K.M; Addison, R.B. Two nuclear polyhedrosis viruses of the Douglas-fir tussock moth *J. Invertebr. Pathol.*, **1970,** 16: p. 196-204.

Jamieson, D. Oxygen toxicity and reactive oxygen metabolites in mammals *Free Radic Biol Med*. **1989**, 7, 87-108.

Lieven, C. J.; Levin, L.A.; Hoegger, M.J. Differential production of superoxide by neuronal mitochondria *BMC Neuroscience* **2008,** 9-4

Luk, E.E.; Culotta, V. C. Manganese Superoxide Dismutase in Saccharomyces cerevisiae acquires its metal co-factor through a pathway involving the Nramp metal transporter, Smf2p *J. Biol. Chem*. **2001,** 276, 47556-47562.

Miller, L. K.; Kaiser, W. J.; Seshagiri, S. Baculovirus Regulation of Apoptosis *Seminars in Virology* **1998**, 8, 445-452.

Murhammer, D.W. Use of viral insecticides for pest control and production insect culture.*Applied Biochemistry and Biotechnology.* **1996**, 59: 199-220.

Murhammer, D. W. Investigation of ROS species generation due to viral infection and its role for propagation of viral infection. 2006 NIH Research Proposal

Murhammer, D. W. Preface. In Methods on Molecular Biology. Baculovirus and Insect Cell Expression Protocols 2nd ed.; Humana Press: 2007b vol. 388.

Murhammer, D. W. Useful Tips, Widely Used Techniques, and Quantifying Cell Metabolic Behavior. In Methods on Molecular Biology, vol. 388: Baculovirus and Insect Cell Expression Protocols 2nd ed; Humana Press: 2007b pp 3-22.

Oda, T.; Akaike, T.; Hamamoto, T.; Suzuki, F.; Hirano, T.; Maeda, H. Oxygen radicals in influenza-induced pathogenesis and treatment with pyran polymer-conjugated SOD *Science.* **1989,** 244, 974-976.

O'Reilly, D. R.; Miller, L. K.; and Luckow, V. A. Baculovirus Expression Vectors: A Laboratory Manual, Oxford University Press: USA, 1993.

Rhiel, M.; Mitchell-Logean, C. M.; and Murhammer, D. W. Comparison of Trichoplusia ni BTI-Tn-5B1-4 (high fiveTM) and Spodoptera Frugiperda Sf-9 insect cell line metabolism in suspension cultures *Biotechnology and Bioengineering.* **1997,** 55, 909-920.

Rohrmann, G.F. *Baculovirus molecular biology*; 2008

Smith, G. E.; Summers, M. D. Analysis of baculovirus genomes with restriction endonucleases *Virology.* **1978,** 89, 517-27.

Spitz, D.; Oberley, L. W. Measurement of MnSOD and CuZnSOD Activity in Mammalian Tissue Homogenates *Current Protocols in Toxicology.* **2001,** 7.5.1–7.5.11.

Swartz, J. R. Advances in Escherichia coli production of therapeutic proteins *Curr. Opin. Biotechnol.* **2001,** 12:195–201

Tomalski, M. D.; Eldridge, R.; Miller, L. K. A baculovirus homolog of a Cu/Zn superoxide dismutase gene *Virology*. **1991,** 184, 149-61.

Turrens J. F. Superoxide Production by the Mitochondrial Respiratory Chain *Bioscience Reports,* **1997,** 17-1

Wang, Y.; Oberley, L. W.; Murhammer, D. W. Antioxidant defense systems of two lipidopteran insect cell lines *Free Radical Biology and Medicine.* **2001,** 30, 1254-1262.

Wang, Y.; Oberley, L. W.; Murhammer, D. W. Evidence of oxidative stress following the viral infection of two lepidopteran insect cell lines *Free Radic Biol Med.* **2001,** 31, 1448-55.

Wong, P. C.; Waggoner, D.; Subramaniam, J. R.; Tessarollo, L.; Bartnikas, T. B.; Culotta, V. C.; Price, D. L.; Rothstein, J.; Gitlin, J. D. Copper chaperone for superoxide dismutase is essential to activate mammalian Cu/Zn superoxide dismutase *Proc Natl Acad Sci USA.* **2000,** 97, 2886–2891.

.